Open Access

Recent Progress in Materials

LIDSEN Publishing Inc.

Review

Review on Material Performance of Carbon Nanotube-Modified Polymeric Nanocomposites

Zhong Hu [1, *], Haiping Hong [2, *]

1. South Dakota State University, Brookings, South Dakota 57007, USA; E-Mail: Zhong.Hu@sdstate.edu
2. South Dakota School of Mines and Technology, Rapid City, South Dakota 57701, USA; E-Mail: Haiping.Hong@sdsmt.edu

* **Correspondences:** Zhong Hu and Haiping Hong; E-Mails: Zhong.Hu@sdstate.edu; Haiping.Hong@sdsmt.edu

Academic Editor: Chih-Ching Huang

Recent Progress in Materials
2023, volume 5, issue 3
doi:10.21926/rpm.2303031

Received: March 21, 2023
Accepted: August 11, 2023
Published: August 16, 2023

Abstract

The chemically functionalized carbon nanotubes (f-CNTs) and hydrogen bonding modified polymer composites (CPCs) exhibit unique chemical, mechanical, electrical, and thermal properties and are emerging as promising materials to achieve extraordinarily high electrical and thermal conductivity, lightweight and anticorrosion, superior strength and stiffness for potential applications in the aerospace and automotive industries, energy conversion, and optical and electronic devices, therefore, attracting considerable research efforts over the past decade. In this review, the fundamentals of the topics on f-CNTs, hydrogen bonding, and CNT directional alignment have been briefly introduced. The research on the electrical, thermal, and mechanical properties have been reviewed. The effects of the CNT morphology, hydrogen bonding, CNT alignment and aspect ratio, and the interactions between the constitutes on the CPC performance is critical to understand the fundamentals and challenges of designing such materials with desired properties and their potential applications. However, to gain a comprehensive and quantitative understanding of the effects of these factors on the performance of CPCs, further studies by computer modeling, especially MD simulations, will be highly needed for effective new/novel material design and development.

Keywords
Material performance; carbon nanotubes (CNTs); functionalized CNTs (f-CNTs); hydrogen bonding; CNT modified polymeric composites (CPCs); CNT directional alignment

1. Introduction

Carbon nanotubes (CNTs) exhibit excellent electrical, thermal, and mechanical properties. CNTs are well-known nanofillers that can be used to produce high-performance CNT-modified polymer nanocomposites (CPCs) [1]. The chemically functionalized CNTs (f-CNTs), incorporating hydrogen bonding and appropriate solvents, facilitate the formation of well-dispersed CNT networks as electronic pathways in polymer nanocomposites [1-7]. Furthermore, it extends the CNT length to enhance the directional performance, together with proper design to create desired properties for desired applications [7]. It has shown promise in aerospace, electrical and automotive industries, energy conversion, ultra-high-strength nanocomposites and high-performance composites, surface engineering, and promising devices in the field of optics and electronics, including energy storage, energy harvesting, mobile phones, optical coatings and antistatic coatings, integrated circuit chips, flexible electrodes in displays, electronic paper, bullet-proof vests, protective clothing, etc. [1-8]. However, polymers are generally considered effective insulators due to their low thermal and electrical conductivity [9]. Research has been actively conducted to improve their electrical, mechanical, and thermal properties, and to develop new functionalities by adding nanoscale fillers to polymeric materials. The choice of nanofillers depends on the properties of the nanocomposite to be designed, the polymer matrix used, their composition, size and shape, their functional groups, their amount, their dispersion in the polymer matrix, and interfacial interactions. Examples of nanofillers include carbon-based nanofillers, layered nanoclays, porous and hollow nanoparticles, nanocellulose, and metallic alloy nanoparticles, to name a few [10, 11]. Among various nanofillers, carbon-based fillers have attracted much attention due to their excellent physical properties.

Carbon materials are unique, and surprise s of the scientific community are constantly escalating their uniqueness, whether it is the structure of benzene, the complex behavior of polymers, or the popular materials such as graphene and its derivatives. The exceptional properties of carbon exist in every phase of matter, which is the most important reason why carbon materials dominate our daily lives. In the past 3-4 decades, carbon nanomaterials have flourished, and nearly 60% of research results in chemistry, physics, materials science engineering, and chemical engineering are directly or indirectly related to carbon nanomaterials. Among various materials, 2D and 3D carbon materials have been rigorously studied in the past 10 years. These materials have made great contributions to modern science, technologies, and industries. Nanomaterials composed of heteroatoms have been extensively explored worldwide, especially in the fields of electrochemical sensing, solar cells, batteries, and catalysis. For energy applications and catalysis, heteroatom-doped carbon nanostructures are considered as potential candidates due to their high surface area, low density, good electrical conductivity, thermomechanical stability, and densely dispersed tunable active sites. Several excellent reviews and books on key carbon materials such as graphite, carbon black, graphene oxide, graphene, porous carbon, and carbon nanotubes composed of nitrogen, sulfur, etc. have been published by renowned research groups around the world. For

example, lanthanum aluminate was used for the first time as a thermal barrier coating material for internal combustion engines, transforming standard engines into low-heat-exhaust engines. The piston crowns, cylinder heads and valves of the engine are coated with lanthanum aluminate with a thickness of about 200 μm to reduce the emission of harmful nitrogen oxides [12]. Carbon-based multilayer films for electronic applications such as charge-trap flash memories, flexible organic resistive memory devices, photovoltaic devices, flexible and transparent electronics, heat sinks in electronic materials, liquid crystal displays (LCDs), thin-film solar cells, flexible touch-screen panels, electronic papers, micro-batteries, electrochemical micro-capacitors, humidity sensors, optoelectronic device, etc. [13]. Furthermore, the development of topological defects induced by heteroatoms doping and its impact on the intrinsic activity of carbon nanostructures has been extensively studied recently. Various active sites have been created in carbon nano-catalysts to enhance their activity [14-17].

Since their discovery, CNTs have been studied as fillers in polymer composites due to their one-dimensional geometry, outstanding mechanical properties, efficient thermal conductivity, and unique electrical properties. As promising materials, their poor solubility in aqueous and organic solvents hinders the application of CNTs. To date, controlled dispersion of CNTs in solutions or polymeric matrices has remained a challenge due to the strong van der Walls binding energy associated with the CNT aggregates. Altering the sidewalls of CNTs may affect the solubility characteristics. The solubility of CNTs can be significantly enhanced by radical grafting, as the large functional molecules facilitate the dispersion of CNTs in various solvents even at low functionalization [18, 19]. Altering the sidewall of CNTs means functionalizing the nanotube. The good part is that it could increase the solubility and dispersion. But the functionalization may break the perfect conjugated structure of nanotube, then decrease physical properties such as thermal, electrical, and mechanical of nanotube. It is always challenging, need to be balanced. Several functionalization methods are chemical [20], electrochemical [21], mechano-chemical [22], and plasmonic [23] in nature. The most common chemical functionalization method is to use strong acid to remove the end caps and shorten the CNT length [6, 24]. In addition, oxide groups were added at the ends and defect sites of CNTs to improve the surface characteristics [25-32].

According to these high expectations, the ultimate practical applications seek CPCs with physical properties closing to the theoretical maximum values of an individual CNT in a polymer matrix. The initial interest in CNT alignment in polymer matrices was described by Ajayan et al. [30], who demonstrated conceptually that the remarkable properties of CNTs could be transferred to a polymer matrix. The physicochemical properties of nanocomposites are mainly determined by the macro- and microstructures generated during the fabrication and processing of the composites. There are several identified factors that affect these properties and the subsequent performance of the resulting nanocomposites. The alignment of CNTs in polymer matrix composites yields more practical properties that fully meet the needs and expectations of innovative applications. Alignment has been recognized as a crucial structural parameter for one-dimensional materials such as CNTs with high aspect ratios. The mechanical properties of the final composite depend on the degree of CNT alignment, particularly when the composite is loaded parallel or perpendicular to the CNT orientation. Alignment can also provide effective conductive pathways for electrons and phonons, which can greatly improve electrical and thermal properties. For composites, highly aligned fillers typically represent dense packing and minimize the lateral degrees of freedom within the bulk matrix; thus, the material is more likely to exhibit similar anisotropic properties to the

individual components. These findings pave the way for the development of various approaches for the incorporation and arrangement of CNTs into host matrices [30-32].

A comprehensive understanding of the impact of composition, hydrogen bonding, CNT orientation, and their interactions on the material system responses for the development of new materials is both scientifically appealing and technologically important. The co-existence of f-CNT structures and networks, matrices, and interfaces from nano- to macro-scales results in these heterogeneous and multifactorial anomalous responses. The broad interest of the scientific community in the development of advanced nanomaterials is evident in the numerous annual international conferences, dedicated journals, and publications on the topic. Examples of potential applications of nanomaterials include:

Hydrogen bonds formed between f-CNTs serve as electronic pathways in highly electrically and thermally conductive erosion-corrosion-resistive nanostructured composite coatings and greases [33, 34]. The areas of applications are in hydro turbine blades, coal-fired boilers, cutting tools, nanofluids (in heat exchangers to increase the heat transfer rate of fluids), the automotive industry, rechargeable batteries, mechanical wear and tear prevention and many specialized applications such as the next generation electric vehicles, super electric motor bearing protection, and electrical contact improvement, to name a few [33, 34]. Hydrogen bonding is believed to be attributed to the best performing samples. With further studies, this finding can be extended to other nanomaterials with functional groups such as OH, COOH, F and NH_2 [8, 33, 34].

Due to their excellent mechanical properties and high aspect ratio, CNTs are envisioned as attractive nanofillers in polymer composites. However, detrimental CNT aggregation is often observed in polymer nanocomposites due to strong van der Waals interactions. Moreover, only limited reinforcement can be obtained due to the low stress transfer between the matrix polymer and the nanotube filler. The mechanical properties of CPCs are still far behind the theoretical predictions. A critical issue in solving this dilemma is to align CNTs in a polymer matrix. One such protocol is electrospinning followed by hot stretching. Another approach is to use functionalization strategy to obtain CNTs with pendant self-complementary hydrogen bonding groups [4, 35-40].

As electronic devices tend to become thinner and more integrated, thermal management becomes a core task in device design and application. Using high thermal conductivity polymer-based composite materials instead of metallic materials as traditional heat dissipation materials has the advantages of lightweight, corrosion resistance, easy processing, and lower manufacturing cost. Hydrogen bonding is a special type of secondary bonding that is widely present/adopted in composites. The effect of hydrogen bonding on thermal transport is found at the electrode/electrolyte interface of solid-state lithium-ion batteries. The structure, orientation and bonding pattern can greatly affect thermal conductivity. As the size of electronic and mechanical devices decreases to the micro- and nanoscale, it becomes more important to predict the thermal transport properties of components [9, 41-55].

CNTs have excellent electrical conductivity and flexibility and are suitable for chemical delivery and touch screen devices for aerospace and defense applications. Understanding the pathways of charge transport within the networks is crucial for developing new functional materials and improving existing devices. The hydrogen-bonded CPCs offer have significantly lower electrical resistance. The hydrogen bonding formed between f-CNTs acts as electronic pathways and dramatically enhances the electrical conductivity of the CPCs [9, 54-61].

Nevertheless, these findings show that very few of the nanocomposite architectures developed

to date achieve their ideal performance, especially in mechanical, electrical, and thermal [31]. A vast portion of research is still struggling to meet target expectations. The challenges of transferring CNT properties to polymer matrix composites and the difficulties of the reproducibility of CNT properties with different preparation methods must be addressed. Incorporating an organized CNT architecture into a well-chosen polymer matrix and engineering the interface between the two constituents is crucial. When considering a CNT/polymer composite, the two critical issues related to CNTs and the CNT-polymer interfacial chemistry are the dispersion and alignment of CNTs in the polymer matrix. While the former is highly desirable to obtain a unform system and a higher CNT density for more capillary distribution in the polymer matrix [33], the latter is of particularly important for anisotropic thermal and electrical properties as well as mechanical strength and fluid transport characteristics. However, in order to enhance the anisotropy of CNTs and attain the optimal performance, it is essential to develop directionally aligned CNT structures and extend the length of CNTs, incorporate hydrogen bonding, in composites and obtain the highest possible to exploit the excellent intrinsic axial properties of CNTs in an actual material [30, 31, 33, 34, 36, 38, 39, 56, 62-64].

In this review, research conducted in the recent decades on the effects of the CPC composition, CNT morphology and aspect ratio, hydrogen bonding, CNT alignment, and interactions among the constitutions on CPC performance will be reviewed to understand how to design such CPCs with desired properties and their potential applications. The research reviews in the relative areas include highly electrically and thermally conductive erosion-corrosion-resistive nanostructured composites, alignment of CNTs in polymer matrix composites for enhanced mechanical, electrical, and thermal applications, thermal management as a core task of a device design and application, and the excellent electrical conductivity and flexibility for chemical transmission and touch screen devices for aerospace and defense applications. Further research method by computer modeling on these topics will be discussed.

2. Concepts of CNT Functionalization, Hydrogen Bonding, and CNT Alignment

The emergence of CNTs has created new opportunities for fabricating polymer composites with potential for a wide range of applications. Numerous significant advances have been attained to date, and more technological challenges await the optimization of the system to fill the gap between expectations and practical performance. Despite this tremendous progress, challenging issues related to CNT functionalization, CNT directional alignment, and assembly within a polymer matrix incorporating hydrogen bonding still remain. This section presents the concepts and fundamentals of these contemporary approaches.

2.1 CNT Functionalization

According to the various technologies are involved in fabricating CNTs/polymer nanocomposites, achieving reproducible, precise and economical nanocomposite remains challenging [65, 66]. It has been reported that functionalization of CNTs can enhance the uniform dispersion of the conductive nanofiller in non-conductive polymers. Azizighannad and Mitra [67] fabricated f-CNTs/polydimethylsiloxane (PDMS) pressure sensors and reported that the functionalization of CNTs can enhance the piezo-resistive behavior of the nanocomposite due to the uniform distribution of the CNTs and the better interfacial interaction between CNTs and the polymer. This

is because of the electrostatic repulsion of the functional groups on the CNTs, which in turn increases the adhesion at the interface between the polymers. This results in enhanced mechanical properties such as initial modulus and thermal degradation compared to the pristine CNTs. McClory et al. [68] analyzed the distribution behavior of f-CNTs through the rheological properties of CNTs/poly (methyl methacrylate) (PMMA) nanocomposites, showing its ability to form a highly rheologically percolated network in PMMA. Although an excellent dispersion with enhanced mechanical properties is achieved, the addition of functional groups degrades the electrical properties of the nanocomposites. This is due to the introduction of sp^3 hybridization inside the nanotubes and the simultaneous loss of the pi-conjugated system of the graphene layer, thereby disturbing the graphitic structure of the nanotubes [69]. The sp^3 hybridization can increase the electronic bandgap and act as defect sites in terms of electron transport through CNTs and lead to a decrease in the tunneling mechanism. It was also noticed that the high interfacial adhesion of the functionalization CNTs between the non-conductive polymers would impede the electron flow between CNTs, i.e., hopping mechanism. Chemical functionalization is based on the covalent linkage of functional entities on the CNT surfaces [67, 70].

Functionalization is to generate functional groups on the surface of CNTs. These functional groups help reduce the long-range van der Waals attraction and increase the CNTs-matrix/solvent interaction and produce a uniform dispersion or lead to CNT solubilization. The effect of CNT functionalization on properties includes enhanced solubility and stability in aqueous and organic solvents. Further functionalized derivatives can be used as molecular linkers to interconnect CNTs, can be soluble in water and capable of trapping water-soluble metal ions and then enhance dispersion of CNTs in a wide variety of polar and non-polar solvents and polymer matrices, etc. [71-77].

There are many well-reported methods for the synthetic functionalization of f-CNTs, which is the primary prerequisite for applying CNTs to any area. Both covalent and non-covalent approaches for functionalization have been reported [76]. Broadly speaking, they can be classified as either exohedral or endohedral, depending on whether the modifications are made on the outer walls of the CNTs [77]. The exohedral functionalization is further subdivided into two categories: (a) covalent functionalization, and (b) non-covalent functionalization, which may be filled with tailored materials to meet specific needs, etc. [77].

In addition to the nanofiller functionalization, there are also many ways to functionalize polymer matrices. Many studies have reported the oxidation of organic synthetic alcohols using polymer-supported reagents. New functional materials have been developed through coordination of polymers, which have a wide range of applications. For the oxidation of alcohols, several oxidizing agents are used. Coordination of polymers via catalyst is more advantageous due to high stability and many active metals. Recently, many nanomaterials have been used as catalysts to increase the oxidation rate in the base matrices. The synthesis of base matrices can also be used to enhance alcohol oxidation [78].

2.2 Hydrogen Bonds

According to IUPAC journal Pure and Applied Chemistry, the hydrogen bonding definition specifies: The hydrogen bonding is an attractive interaction between a hydrogen atom from a molecule or a molecular fragment X-H in which X is more electronegative than H, and an atom or a

group of atoms in the same or a different molecule, in which there is evidence of bond formation [79]. Such an interacting system is generally denoted as Dn-H···Ac, where Dn denotes a more electronegative "donor" atom or group, and Ac denotes another electronegative atom with a lone pair of electrons – hydrogen bond acceptor, the solid line denotes a polar covalent bond, and the dotted or dashed line indicates the hydrogen bond. Hydrogen bonds can be intermolecular or intramolecular. The energy of a hydrogen bond depends on the geometry, environment, and the nature of the specific donor and acceptor atoms and can vary more than two orders of magnitude between about -0.2 to -40 kcal/mol [80]. This makes them somewhat stronger than van der Waals interactions, but weaker than fully covalent or ionic bonds. This type of bond can occur in inorganic molecues such as water and organic molecules such as DNA and proteins.

Hydrogen bonds are responsible for holding materials like paper and felted wool together and cause individual sheets of paper to stick together when they get wet and then dry. Hydrogen bonding is due in part to the high electronegativity difference between a hydrogen atom and an atom of one of the elements fluorine (F), oxygen (O), or nitrogen (N) [81, 82]. Since the σ bond that causes this is linear and polar, a positive charge will be exerted through the hydrogen atoms in a direction parallel to the bond. A second vital requirement for hydrogen bonding to occur is the presence of a lone pair on the local species. The negative charge of a lone pair of electrons acts in a direction away from the atom with which it is associated. Combining these factors, it is easier to see that due to charge attraction, the strength of the hydrogen bond will be the strongest when the two forces act in as different directions as possible, which is the case when the original electronegative atom, the hydrogen atom, the atom with lone pair, and the lone pair itself, are all aligned with one another [72, 83-87]. A schematic diagram of H-bond examples is shown in Figure 1.

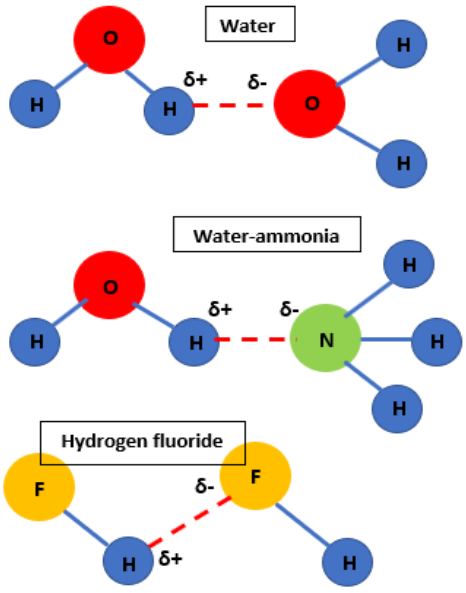

Figure 1 Examples of hydrogen bonds.

Compared with other similar structures, hydrogen bonding is responsible for many physical and chemical properties of compounds of N, O and F that seem unusual. It also plays an important role in the structure of both synthetic and natural polymers. It plays an important role in determining the three-dimensional structures and properties adopted by many synthetic and natural proteins. Compared to the C-C, C-O, and C-N bonds that make up most polymers, hydrogen bonding is much

weaker, only about 5%. Thus, hydrogen bonding can be broken by chemical or mechanical means while retaining the basic structure of the polymer backbone. This hierarchy of bond strengths (covalent bonds, which are stronger than hydrogen bonds, are stronger than van de Waals forces) is key to understanding the properties of many materials [88].

2.3 CNT Directional Alignment

Materials with high electrical and thermal conductivity as well as lightweight are highly desired for applications in aerospace and electronics [56]. The most common materials used for these applications are metal-based and conductive polymer-based materials. However, metal-based materials are heavy, and polymer-based materials cannot be used in ultra-high temperature environments. Although some advanced ceramics have applications at high temperatures, they are still not ideal choices for aerospace applications due to their high specific weight. On the other hand, carbon materials such as CNTs, graphene, fullerene, graphite, carbon nanofibers and carbon/carbon composites are lightweight materials that can not only be used at high temperatures (non-oxidizing environments), but also have excellent conductive properties. Carbon materials have emerged as suitable candidates for lightweight and high conductive aerospace applications. The crystal-packed structure of CNT assemblies can limit contact resistance and facilitate charge transfer among individual nanotubes and bundles of CNT assemblies. For example, the electrical conductivity of the composite material reaches 7.70×10^2 $S \cdot m^{-1}$ through the vapor-phase infiltration of carbon to densify the aligned CNT films [87]. Recently, an electrical conductivity of $\sim 1.3 \times 10^6$ $S \cdot m^{-1}$ for aligned CNT sheets was achieved by using mechanical stretching of CNT sheets and surface chemical iodine doping [51, 87]. A schematic diagram of CNT aligning and assembling under electric field is shown in Figure 2 [88].

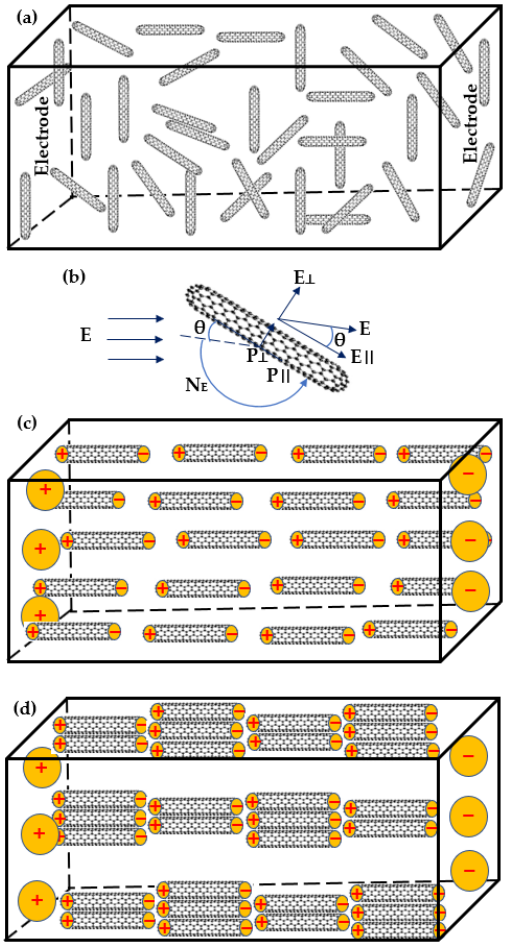

Figure 2 Schematic model of CNT aligning and joining in liquid medium in the direction of electric field. (a) Initial state. (b) Schematic diagram of a polarized CNT in an electric field. (c) CNT aligning in the electric field direction. (d) The polarized CNTs align and assemble into a network.

The physicochemical properties of nanocomposites are primarily dictated by the macro- and microstructures generated during the fabrication and processing of the composites. There are many identified factors that affect these properties and the subsequent performance of the resulting nanocomposites. The alignment of CNTs in polymer-based composites yields more practical properties that perfectly meet the needs and expectations of innovative applications [31].

Since the CNT alignment has a significant impact on the properties of the resulting polymeric composites, tailoring the degree of CNT alignment to the composite is a fundamental issue, particularly during the synthesis stage of the material [31]. In general, CNTs can be aligned horizontally or vertically to the surface of the polymer composite films, which largely depends on the application of the resulting composite. It is generally accepted that vertically aligned configurations are more challenging and complex to achieve than horizontally aligned CNTs [31]. In most established methods, an external force such as a magnetic or electric field, mechanical stretching, or shear force is applied to orientate the CNTs [31].

Based on the predictability of the nonlinear stress-strain constitutive relationships, elastic hysteresis, hygro-thermo-mechanical properties, and elastic damping response of CNT-modified polymeric composites, there are many studies based on the stochastic nature of the constituent

parameters, elastic energy release approach based on stick-slip analytical method, and multi-scale computational method based on finite element method for understanding the effects of the CNT alignment, constituent and process parameters on the performance of the CNT-modified polymeric matrix composites [89-93].

Through a fundamental understanding of the strongly dependent processing–structure–performance relationships, the creation of aligned CNT/polymer multi-functional nanocomposites with controlled hierarchical structures offers a wide range of applications [31]. Aligned CNT/polymer nanocomposites fabricated by various methods exhibit many outstanding properties that have been extensively explored for applications in electronic nanodevices, chemical and biological sensors, actuators, and energy sources [31].

The incorporation of CNTs into polymer matrices offers a viable route to extend the interesting properties of CNTs from the nanoscale to the macroscopic level. However, the most important limitation for practical applications in the fields of composite science and technology comes from the fact that randomly oriented CNTs embedded in bulk samples exhibit much lower performance (especially in mechanical, electrical, and thermal) than expected [31]. Therefore, it has been proposed to incorporate an organized CNT architecture (align CNTs) into a carefully selected polymer matrices and engineer the interfaces between the two constituents to extend the interesting properties of CNTs from the nanoscale to the macroscale [62, 87, 88, 94-99].

3. Research Summary on f-CNTs, CNT Alignment, Hydrogen Bonding, CPCs

Understanding how the addition of CNTs to polymer composites and how to effectively transfer the unique properties of CNTs from the nanoscale to the macroscale into CPCs is vital which is related to the mechanical, thermal, and electrical performance of CPCs. The primary focus of our review on the relative topics is to understand why the thermal, electrical, and mechanical properties of polymers can be improved using nanofillers. The CPC material design involves manipulating the material system composition, including chemically f-CNTs, hydrogen bonding, various structures of CNTs (chirality, number of wall layers, aspect ratio, etc.), and interactions among the constitutes and matrices based on chemical physics and materials science.

3.1 Electrical Properties

Electrical resistivity and/or conductivity is an important property of materials. Conductivity and resistivity are inversely proportional to each other. Electrical conductivity is based on electrical transport properties. Polymers offer distinguished advantages as dielectrics over traditional inorganic materials. Suitable applications may vary, for example, polymers with a low dielectric constant are ideal for communication cable insulation. The electrical characteristics of CPCs have been receiving much attention. However, evaluating the electrical conductivity of CPCs by experiments for the development of CPCs with desired properties is an expensive and inefficient method. It is certainly more efficient and economical to preform computational evaluations by using mathematical models of the physics governing charge transport in CPCs. To obtain the electrical conductivity of the CPC, Figure 3 depicts the geometrical configuration of the computational modeling domain of a specimen, where the test voltage, V_{test}, is applied throughout the cross-sectional area A of the entire specimen length L_0 [100]. Therefore, the electrical conductivity can be calculated by

$$\sigma = \frac{J}{E} = \frac{\left(\frac{I}{A}\right)}{\left(\frac{V}{L_0}\right)} = \frac{1}{\rho} \quad (1)$$

where σ and ρ are conductivity and resistivity, respectively. *E* and *J* are the electrical field and the current density, respectively.

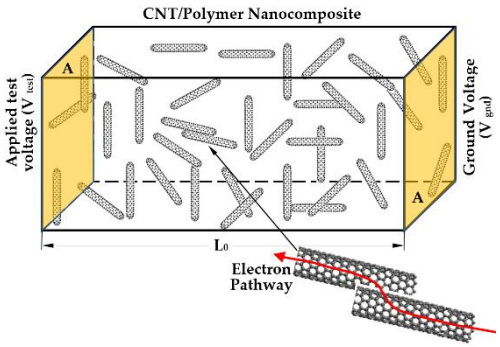

Figure 3 Schematic model of CPC electrical property test.

An interesting finding is that the voltage distribution on the CNTs belonging to the percolation network follows a nearly linear distribution from top to bottom. Since the uniformly distributed CNTs are interconnected by electron tunneling, it is likely to form a linear voltage distribution across the entire CNT/polymer composite region. Otherwise, more locations/points may need for higher accuracy to take the measurements along the length of the model. It was found that the electrical properties of the CPCs depended on the state, geometry, and processing of CNTs. Table 1 summarizes some electrical properties of CPCs with various polymer matrices, different morphological CNT fillers and aspect ratios, fabrication processes, and percolation thresholds [57].

Table 1 The electrical properties of some CPCs from literatures.

Matrix	CNTs Filler	Aspect Ratio	Fabrication Process	*Electrical Conductivity/Resistivity	Percolation Threshold	Ref.
Polyester	Multi-walled CNTs (MWNTs)	D = 50 nm, L = 10-20 μm	Stirring	3.9×10^{-2} $(\Omega \cdot m)^{-1}$	0.6%	[101]
Polyurethane	Amino-CNT	D = 8-15 nm, 50 nm	Co-coagulation and compression molding method	$<4.48 \times 10^{-6}$ $S \cdot cm^{-1}$	0.337 vol%	[102]
Epoxy	SWNTs	D = 1.34 nm, L = 1-10 μm	Solvent processing in acetone	$\sim 4.74 \times 10^{6}$ $S \cdot cm^{-1}$	0.2~0.5 wt.%	[103]
PVDF	MWNTs		Melting mixing and compression molding	$\Delta R/R_0$ ** = 84.7%	1.25-8 wt.%	[104]
PMMA	MWNTs	ID = 5-10 nm, OD = 60-100 nm, L = 0.5-500 μm	Solvent mixing in chloroform	1.6-107 Ω/sq.	0.8-1%	[105]
Epoxy	MWNTs	D = 10-20 nm, L = 10-15 μm	CNTs treated with nonionic surfactant	$>10^{6}$ $S \cdot cm^{-1}$	0.05-0.08 wt.%	[106]
PMMA	SWNTs	D = ~6.9 nm, L = ~310 nm	Hot pressing as coagulated	6.5×10^{-11} $S \cdot cm^{-1}$ (random) to 2.7×10^{-3} $S \cdot cm^{-1}$ (aligned)	2 wt.%	[107]
PA	SWNTs	D = 1.2-1.8 nm, L/D = 100-1000	Electric arc discharge	1.2×10^{3} - 1.7×10^{3} $\Omega \cdot cm^{-1}$	9.3 vol.%	[108]
Polyamide film	SWNTs		BuckyPearls™ from Nanotechnologies Inc.	10^{6} ~3.2×10^{7} $\Omega \cdot \Upsilon^{-1}$	0.1-0.2 wt.%	[109]
PEDOT/PSS	SWNTs		Doped VP	3 $\Omega \cdot cm^{-1}$	2 wt.%	[110]
PEDOT/PSS	SWNTs		Doped VP	1.2×10^{3} $\Omega \cdot \Upsilon^{-1}$	1 wt.%	[110]

glycerol						
PEDOT	SWNTs-buckypaper		HiPCO and Electric arc discharge	~160 $\Omega \cdot \Upsilon^{-1}$		[111]
N/A	SWNTs-buckypaper	By Iljin Nanotech., Inc.	Acid treatment	40-70 $\Omega \cdot \Upsilon^{-1}$	100%	[112]
Poly(allylamine hydrochloride)	MWNTs	D = 10-30 nm	CNTs by CVD, f-CNTs by oxidation	10^4 Ω	8 wt.%	[113]
Polyelectrolyte (cotton)	SWNTs & MWNTs		Dipping technique	20 $\Omega \cdot cm^{-1}$	>0.002 wt.%	[114]
Cellulose paper	CNTs			0.53 $\Omega \cdot cm^{-1}$	8.32 wt.%	[115]
PE	MWNTs	Film t = 250 nm	Inert particulate fillers CaCo3, talc and wollastonite	5×10^4 $\Omega \cdot \Upsilon^{-1}$	0.8 vol.%	[115]
Cellulose	Graphene and CNTs	D = ~20-60 nm, L = ~a few μm	Fluorinated CNT/Nanofibrillated	Film 10^{10} Ω·cm	35 wt.%	[116]
P(VDF-TFE)	SWNTs + rGO	D = 1.2-2.2 nm, L/D = 10^3-10^4.		12.2 $S \cdot m^{-1}$	1 wt.%	[117]
DMA(b)	CVD-MWNTs	From Hyperion Catalysis Int., Inc.	In situ polymerization	~10 Ω·cm	1-15 wt.%	[118]
BP	SWNTs	D ~5.6 nm, L ~547 nm	Sheets	1.7-3 times↑[§]	48 wt%	[119]
(BPDA/PDA) Polyimide	CVD-CNTs	D ~10 nm, L ~700 μm	CVD + aligned	10^{-6}-183.3 S/cm, 10^{18} times↑	4.5 wt.%	[120]
HDPE	MWNTs	D ~9.5 nm, L = 1.5 μm	Compression molding + blown film extrusion	~10^8-10 Ω·cm	10 wt.%	[121]
PP	CVD-MWNTs	D = 10-100 (ave.25.8) nm, L = 1.5-9.5 μm	Melt mixing and extrusion	0.001-0.01 S/cm	15 wt.%	[122]

Epoxy	MWNTs	D = 8-15 nm, L ~50 μm	Sonication and stirring	10^{-16}-0.16 S/cm by 15 orders	1.5 wt.%	[123]
EG/MPD/BDO	MWNTs	DO = 8-15 nm, L ~50 μm	Solution mixing and sintering	1.6×10^{-5} S/cm	1.5 wt.%	[124]
TPU-acetone	MWNTs	D ~9.5 nm, L ~1.5 μm	Sonication	~1000-10000 S/m	10-60 wtwt.%	[125]
CPU	MWNTs	DO ~20 nm, L = 5-10 μm	Sonication and stirring	1.1×10^{-4} S/cm	-0.65 wt%	[126]
Epoxy	MWNTs		Tannic acid and PEI/MWNTs	Remarkably enhanced	0.4 wt.%	[127]
Epoxy	MWNTs	D ~9.5 nm, L ~15.5 μm	Epoxidation and chemical treatment	1.5×10^{-15} to 5.7×10^{-3} S/cm	7.5-16 wt.%	[128]
PEEK	CVD-MWNTs	DO = 13-16 nm, DI = 4 nm, L = 1-10 μm	Shear mixing by calendaring technique	From 10^{-14} to 10^{-7}, 10^{-4} (S/cm)	3.5, 10 wt.%	[129]
PEEK	MWNTs	D ~15 nm, L ~1-10 μm	Mechanically mixed with PEEK and then melt	From 10^{-14} to $>10^{-5}$ (S/cm), contact resistance from 10^{19} to 10^{10} Ω	1, 10 wt.%	[130]
Epoxy	CNTs	SWNT: D = 0.8-2 nm, L = 5-30 μm, MWNT: D = 10-20 nm, L = 10-30 μm	f-CNT by hydroxyl	Up to 0.1 S/cm	0.8 wt.%	[54]
PDMS	S-MWNT(L/D~60), M-MWNT(L/D~173), L-MWNT(L/D~400)	S-MWNT:D = 12.5 nm M-MWNT:D = 12.6 nm	Three-roll milling process	75-310 S/m	10 wt.%	[55]

PS	SWNTs/MWNTs	L-MWNT:D = 17.0 nm SWNT:D <1 nm MWNT:D >20 nm	Latex-based process	10^{-10}-0.1 S/m 10^{-10}-~2 S/m	2.0 wt.% 4.0 wt.%	[60]
PMMA	MWNTs	D = 2-30 nm, L <1-10 μm	f-CNT by carboxylic acid	Up to 10^{11}times↑	0.5 wt.%	[67]
SBS	CNTs	SWNT:D~1.4 nm, L = 0.5-3 μm, MWNT:D~10-16 nm, L~10 μm	f-CNT by covalent/non-covalent	10^{-12} up to >10^{-2} S/m	2 wt.%	[68]
Grease	Hydroxyl MWNT-OH		Petro-Canada N650HT oil	10.0-7880 Ω·cm	4.5-8.4 wt.%	[36]
Polyurethane	MWNT-OH	D = 20-40 nm, L >>[§§] aspect ratio	75%polyurethane/25%ethanol	6.8 Ω·cm	4.5 wt.%	[35]

* Note: unit for electrical conductivity S/cm or $\Omega \cdot \Upsilon^{-1}$, electrical resistance Ω·cm.

** Note: the electric resistance change rate.

[§] ↑ - indicating increasing.

[§§] >> - indicating much larger than.

3.2 Thermal Properties

For the thermal property measurements, the schematic diagram is similar to Figure 3, where the heat (phonons) flows through the CNTs instead of electrons through the CNTs, with heat flux applied on one side (hot region) and heat sink applied on the other side (cold region). The heat flux J can be calculated by

$$J = \frac{dq}{2Adt} \tag{2}$$

where dq is the heat added to the hot region duing the time incremental dt, and A is the cross-sectional area over which the heat is transferred. Then the thermal conductivity *k* can be calculated as

$$k = \frac{J}{\partial T/\partial L} = \frac{dq}{2Adt(\partial T/\partial L)} \tag{3}$$

The coefficient of thermal expansion α(T) can be calculated as

$$\alpha(T) = \frac{1}{L_0}\frac{dL}{dT} \tag{4}$$

where L_0 is the original length of the specimen in the direction of heat transfer and *T* is the temperature in the specimen. Table 2 summarized some thermal properties of CPCs with various polymer matrices, different morphological CNT fillers and aspect ratios, fabrication processes and percolation thresholds.

Table 2 The thermal properties of some CPCs from literatures.

Matrix	CNTs Filler	Aspect Ratio	Fabrication Process	*Thermal Conductivity	Percolation Threshold	Ref.
Cellulose	Graphene and CNTs	D = ~20-60 nm, L = ~a few μm	Fluorinated CNT/Nanofibrillated	Film 14.1 $W \cdot m^{-1} K^{-1}$	35 wt.%	[116]
iPP & sPP	CVD-MWNTs	D <10 nm, L = 5-15 μm	Acid-treated MWNTs	10%↑	iPP 3.5 wt.% sPP 2.5 wt.%	[119]
(BPDA/PDA) Polyimide	CVD-CNTs	D ~10 nm, L ~700 μm	CVD + aligned	0.027-18.4 W/(mk), 681×↑	0.13 wt.%	[120]
Epoxy	MWNTs	D ~9.5 nm, L ~15.5 μm	Epoxidation and chemical treatment	>10×↑	7.5-16 wt.%	[131]
PVDF	s-MWNTs/GE (1:1)	DO ~10 nm, L = 10-20 μm	3-dimensional network structure	0.19-1.35.11 711.1%↑	10% of s-MWNT/GE	[132]
Nano grease	SWNTs/MWNTs/MWNT-OH	D = 20-40 nm, L = 10-30 μm	f-MWNT by hydroxyl	163.3%↑, 545.9%↑	5 wt.%, 12 wt.%	[50]
PEG400-fluids	MWNT-OH/CNFs/BWNTs	From Lower Friction Inc.	f-MWNT by hydroxyl	89.7%↑, 73.1%↑ @2wt%CNF/2wt.	7.5 wt.%	[51]
PU fluids	CNFs/Bo nitrde nanoparticles	From Lower Friction Inc.	OH-BN by H-bonds	390%↑@35wt%BN, 480%↑@20wt%BN + 5we%CNF	0-20 wt.% CNFs	[52]
Epoxy	CNTs	SWNT:D = 0.8-2 nm, L = 5-30 μm, MWNT:D = 10-20 nm, L = 10-30 μm	f-CNT by hydroxyl	0.22-0.40	0.8 wt.%	[54]
PDMS	S-MWNT(L/D~60), M-MWNT(L/D~173), L-MWNT(L/D~400)	S-MWNT:D = 12.5 nm, M-MWNT:D = 12.6 nm, L-MWNT:D = 17.0 nm	Three-roll milling process	0.41-0.47	10 wt.%	[55]

*Note: unit for thermal conductivity W/(m·K).

3.3 Mechanical Properties

For the mechanical property measurements, the schematic diagram is similar to Figure 3, where the stresses are transmitted through the CNTs instead of electrons through the CNTs. The model/specimen can be defined as a cubic shape whose dimensions can be defined by the initial length L_0 and the cross-sectional aera A, and the tensile force F or tensile stress can be applied on the area, so that a uniaxial tensile test can be performed on the model. The Young's modulus of the CPC specimen can be calculated by

$$E = \frac{\Delta\sigma}{\Delta\varepsilon} = \frac{F}{A}\frac{L_0}{\Delta L} \tag{5}$$

where Δσ and Δε are the incremental stress and strain, respectively, in the elastic deformation region (the stress and strain data at the beginning part of the uni-axial tensile test). ΔL is the incremental length of the specimen in the tensile direction after the tensile force is applied. The Poisson's ratio can be calculated by

$$\upsilon_{ij} = -\frac{\varepsilon_j}{\varepsilon_i} \tag{6}$$

where ε_i and ε_j are the strains in the tensile force applied direction and the lateral direction, respectively.

Other mechanical properties can be determined accordingly according to American Society for Testing and Materials (ASTM) standards. Table 3 summarizes some mechanical properties of CPCs with various polymer matrices, different morphological CNT fillers and aspect ratios, fabrication processes, and percolation thresholds.

Table 3 The mechanical properties of some CPCs from literatures.

Matrix	CNTs Filler	Aspect Ratio	Fabrication Process	Mechanical Properties	Percolation Threshold	Ref.
Polyelectrolyte (cotton)	SWNTs & MWNTs		Dipping technique	E = 0.140 to 0.342 , *TS = 41.6 to 87.8	>0.002 wt.%	[114]
Methyl/ethyl P(MMA-co-EMA)	CVD-MWNTs		f-CNT by Octadecylamine. Solution casting	E 2.3 135% ↑, TS 73.4 49% ↑	10 wt.%	[133]
Epoxy	SWNTs	L = ~0.25 µm	f-CNT by large organic groups. Solution casting and curing	E = 2.03-3.40 TS = 83-104, 30-70% ↑ #ε_f = 17-72%	1-4 wt.%	[134]
Polyamide 6 (PA6)	SWNTs	D = ~5 nm, L = 0.5-2 µm	f-CNT by SWNT-COOH	E = 0.44-1.20, TS = 40.9-92.7	0.1-1.5 wt.%	[135]
Poly(vinyl alcohol) PVA	SWNTs	D = 0.80-1.26 nm	f-CNT by hydroxyl. Solution casting	E = 2.4-4.3 79% ↑, TS = 69-107 47% ↑	Up to 0.8 wt.%	[136]
PVA	CVD-MWNTs		f-CNT by ferritin protein. Solution casting	E = 3.4-7.2 100-110% ↑	1.5 wt.%	[137]
PC	CVD-MWNTs	D = ~30 nm	f-CNT by Epoxide. Solution casting and injection molding	E = 2.0-3.8	5 wt.%	[138]
PMMA	MWNTs	D = 20-50 nm, L = 5-20 µm	f-CNT by coated PMMA/PECVD. Melt mixing and extrusion	E = 2.7-2.9	3 wt.%	[139]
PVC	CVD-MWNTs	D = ~14 nm	f-CNT with CPP. Solution casting	E = 0.56-0.9	1 wt.%	[140]
PS	CVD-MWNTs	D = ~14 nm	f-CNT with CPP.	E = 1.48-2.63	1 wt.%	[140]

			Solution casting			
Copolymers of PSVPh	CVD-MWNTs, HiPCO-SWNTs	From Carbon Nanotechnologies, Inc.	f-CNT by carboxylic acid. Solution cating	E = 1.5-2.1, TS = 16-27, ε_f = 1.2-1.6%	5 wt.%	[141]
PU	CVD-MWNTs	From Iljin Nano Tech, Korea	f-CNT by carboxylic acid. Solution casting	E = 0.05-0.42 740% ↑, TS = 7.6-21.3 180% ↑	Up to 20 wt.%	[142]
Sythetic spider silk	SWNTs	From Carbon Solutions Inc.	f-CNT by octadecylamine. Solution casting	E = 1.58-1.92 21.5% higher	~0.125 wt.%	[143]
PAMAM	SWNTs	From Sigma-Aldrich	f-CNT by epoxy. Solution casting and curing	E = 2.76-3.49, TS = 64.1 – 85.3, **K_{IC} = 0.56 – 0.75 (MPa $m^{1/2}$)	1 wt.%	[144]
Kevlar	CVD-MWNTs	D = 12-37 nm	f-CNT by PVC. Solution casting	E = 1.5-2.4 70% ↑, TS 50% ↑	2 wt.%	[145]
Epoxy	CVD-MWNTs	D = 40-60 nm, L = 5-15 µm	f-CNT by TETA. Cast molding	E = 1.56-2.4 38% ↑, TS 30% ↑	0.6 wt.%	[146]
PS	CVD-MWNTs		f-CNT by butyl. Solution casting	E = 1.29-1.63 25% ↑, TS 50% ↑	0.25 wt.%	[147]
Polystyrene	MWNTs	D = ~30 nm, L = 15-50 µm	Solution casting	E = 1.19-1.69 36-42%↑, TS = 12.8-16.0 ~25%↑	1 wt.%	[148]
PVA/PVK films	MWNTs	L/D = 40-800	Solution casting	E 180%↑, ***H 160%↑ in PVA; E 280%↑, H 200%↑ in PVK	1 wt.%	[149]
s-PS films	CVD-MWNTs	D = 40-140 nm, L = 2-10 µm, L/D	Melt processing	E = 0.52 × 10^{-3} - 3.54 × 10^{-3}	15 wt.%	[150]

		= ~100				
PS films	MWNTs	D = 30 nm, L = 50-55 µm, L/D = 1471	Melt processing	E double	2.5 vol.%	[151]
High density PE	CVD-MWNTs	D = 15 nm, L/D >100	Melt processing	E = 0.98-1.35	1 wt.%	[152]
Poly(vinyl alcohol) PVA	SWNTs, DWNTs, NMWNTs OHWNTs OMWNTs AMWNTs	D = 9 nm, L >10 µm; D = 2.5 nm, L = 2.2 µm; D = 14 nm, L = 2.1 µm; D = 15 nm, L = 1.6 µm; D = 16 nm, L = 3.8 µm; D = 24 nm, L = 0.8 µm;	Melt processing	E = 2-3.6	1 wt.%	[153]
CI-PP	CVD-MWNTs		Melt processing	E = 0.22-0.68; E × 3.1, TS × 3.9, K × 4.4	1 wt.%	[154]
PVA	CVD-MWNTs		Melt processing	E = 1.9-7.04; E × 3.7, TS × 4.3, K × 1.7	1 wt.%	[154]
PS	Annealed SWNTs		Melt processing	E = 2.23-2.275	2 wt.%	[155]
P(VDF-TFE)	SWNTs + rGO	D = 1.2-2.2 nm, L/D = 10^3-10^4.		E = 0.3787, 14% ↑	1 wt.%	[117]
Polyethylene (PE)	MWNTs	D = 40-70 nm, L = ~µms	Melt processing	E = 0.682-1.24 82% higher,	5 wt.%	[156]

PHB	SWNTs	D = 1.2-1.4 nm, L = 5-100 nm	Melt processing	E = 5.66-11.74, H = 0.31-0.35	10 wt.%	[157]
PHO	SWNTs	D = 1.2-1.4 nm, L = 5-100 nm	Melt processing	E = 0.12-0.53, H = 0.00056-0.00137	10 wt.%	[157]
PMMA	Arc-MWNTs	From Laboratory Mixing Molder (Atlas, USA)	In situ polymerization	E = 0.73-1.63	17 wt.%	[158]
PS	CVD-MWNTs	CNT alignment by extruding	In situ polymerization	E = 2.3-2.6, E, @Sy and TS 5 times ↑	5 wt.%	[159]
DMA(b)	CVD-MWNTs	From Hyperion Catalysis International, Inc.	In situ polymerization	E = 0.8-1.04	15 wt.%	[118]
PMMA	CVD-MWNTs	Oriented by extrusion	In situ polymerization	E = 2.7-3.7 28%↑, K 170%↑, Sy 25%↑	1 wt.%	[160]
PA6 blend	CVD-MWNTs	MD simulation	In situ polymerization	E = 2.6-4.2	12.5 wt.%	[161]
Nylon	CVD-MWNTs	Varying, D ~20 nm, L ~10 s µm	In situ polymerization	E = 0.4-1.24 214% ↑, Sy 162% ↑	2 wt.%	[162]
PP	Arc-SWNTs	D = 1.3-1.5 nm, 7-12 nm	Melt processing	E = 0.12-0.53	10 wt.%	[163]
PBO	SWNTs	D ~0.95 nm,	In PPA polymerization	E = 138-167, TS = 2600-4200 50%↑,@@ CS = 350-500	10 wt.%	[164]
PMMA	Arc-MWNTs	Provided by MER Corporation	f-CNT by chemical	E = 1.5-2.5 1135%↑	1 wt.%	[165]
PMMA	MWNTs	D = 16.6 nm, L =	f-CNT by CVD MWNT-	E = 0.71-1.38 94%↑,	0.3 wt.%	[166]

		1.2 μm	OH	TS 360%↑, K 1282%↑, ε_f 526%↑		
Polyimide	SWNTs	D = 1-2 nm	Debundling of SWNTs	E = 3.8-7.2	1 wt.%	[167]
Benzyl peroxide-PP	SWNTs		f-CNT by benzoyl peroxide	E = 0.452-1.372 133.7%↑, TS 173.1%↑,	7.5 wt.%	[168]
iPP & sPP	CVD-MWNTs	D <10 nm, L = 5-15 μm	Acid-treated MWNTs	E = 1.2-1.65 25%↑ iPP, E = 0.38-0.635 66%↑ sPP	0.1(iPP)-0.4(sPP) wt.%	[169]
PVA	SWNTs	D = ~0.8 nm	Soak in polymer soltion sheets	E = 2.3-6.9 3×↑, TS 9×↑, K 9×↑	~70 wt.%	[119]
Resin	SWNTs/MWNTs	L = ~1 mm, L/D = ~10,000-100,000	f-CNT by m-CPBA	E = 2.55-15.10 429%↑,	31.3 wt%	[170]
PC	SWNTs	D ~5.6 nm, L ~547 nm	Sheets	E = 2.29-5.08 220%↑, TS6.49-19.7	48 wt%	[171]
PU	SWNTs	HiPCO SWNTs, high L/D	f-CNT by PEG-SWNT	E = 0.004-3.4, K 240 ×↑ at 40 wt.%	100%	[172]
PC	SWNTs	D = 6-14 nm, L ~547 nm	Multi-step dispersion	E = 1.8-6.2 3.4×↑	20 wt.%	[173]
PA6	MWNTs	D = 50-80 nm, L = 5-20 μm	f-CNT by diamine and acid modified	E 123.9%↑, Sy 115.3%↑ at 1 wt.%	0.5-8.2 wt.%	[174]
Poly(1-butene) PB	CVD-MWNTs	D = 10-20 nm, from Shenzhen Nanotech Port Co. Ltd.	PP-g-MWNTs	E = 0.726 91%↑, Sy = 0.0282 83%↑, TS = 50.1 61%↑, K = 88.9 67%↑	1.5 wt.%	[175]
PE	CVD-MWNTs	D = 10-20 nm, from Shenzhen	f-CNT by surfuric and nitric acid, PE-g-	E 75%↑, TS 33%↑, K 61%↑	1.5 wt.%	[120]

		Nanotech Port Co. Ltd.	MWNTs			
Natural rubber (NR)	CVD-CNTs	D = 20-50 nm, L = 0.1-1 μm	pretreated by HF + with HRH bonding systems	E = 1.8-12.5, TS = 7.2-24.8, H = 41-63	25 phr	[176]
(BPDA/PDA) Polyimide	CVD-CNTs	D ~10 nm, L ~700 μm	CVD + aligned	E 12×↑, TS 2.73 ×↑		[177]
Shell EPSON 828 epoxy	CVD-MWNTs, SWNTs	D ~15 nm, L/D ~1000	Melt processing + polymer grafting + alignment	E = 4.5-29, TS = 41-4200	0.6 vol.%	[177]
PMMA	(5,5) CNTs	L/D = 7.23, 14.21, 22.01, ∞	By MD simulation	E = 3.90, 4.73, 6.85, 46.73 MPa	1-7 wt.%	[121]
PC	MWNTs	D = 10-15 NM, l = 1.6 μm	Grafting extrusion, MWNTs-OH, PC-g-MWNTs	E = 1.45, TS = 61 26%↑	2 wt.%	[122]
HDPE	MWNTs	D ~9.5 nm, L = 1.5 μm	Compression molding + blown film extrusion	E = 2.3 163%↑, TS = 18, 34%↑ TS 239%↑	8 wt.%	[178]
PP	CVD-MWNTs	D = 10-100 (ave.25.8) nm, L = 1.5-9.5 μm	Melt mixing and extrusion	E = 0.37, TS = 47 38%↑	15 wt.%	[123]
PLA/ESO	Cu-MWNTs	from Grafen Chemical Industries	Mechanical stirring and sonication	E = 0.97 33%↑, TS = 0.8 54%↑	2 wt.%	[125]
Epoxy	MWNTs	D = 8-15 nm, L ~50 μm	Sonication and stirring	E = 1.57-1.97, TS = 135-151↑	1.5 wt.%	[179]
EG/MPD/BDO	MWNTs	DO = 8-15 nm, L ~50 μm	Solution mixing and sintering	E = 0.025-575, TS = 8.4--63	1.5 wt.%	[180]
UHMWPE	CCVD-MWNTs	D ~9.5 nm, L	Solution and sonicated	E = 0.25 20%↑, TS =	0.02-10 wt.%	[181]

		~1.5 μm		22 37%↑		
WBPU	Amide-MWNTs	D = 40-60 nm, L ~20 μm	Sonication and stirring	E = 0.07 10%↑, TS = 12 20%↑	0.5 wt.%	[126]
TPU-acetone	MWNTs	D ~9.5 nm, L ~1.5 μm	Sonication	E = 1.27 950%↑, TS = 41 20%↑	35 wtwt.%	[182]
CPU	MWNTs	DO ~20 nm, L = 5-10 μm	Sonication and stirring	E = 14 100%↑	-1.5 wt%	[183]
PMMA	Acid-SWNTs	DO = 5-10 nm, DI = 1-5 nm, L = 5-30 μm	Solution mixing, COOH-SWNTs	E ~1.3 188%↑, TS = 30 200%↑	5 wt.%	[184]
Epoxy	ZnO-MWNTs		Sonication	E = 3.6 51%↑, TS = 61 20%↑	1.7 wt.%	[124]
PP	CNTs	D ~9.5 nm, L ~1.5 mm	Solid phase molding	TSC 133%↑, EC 65%↑, TST 74%↑, ET 130%↑	5 wt.%	[127]
Epoxy	MWNTs		Tannic acid and PEI/MWNTs	K = 40.51 154%↑, TS = 80.83 148%↑	0.4 wt.%	[128]
Epoxy	MWNTs	D ~9.5 nm, L ~15.5 μm	Epoxidation and chemical treatment	E = 8.4 144%↑, TS = 203 50%↑	7.5-16 wt.%	[131]
Epoxy	a-SWNTs	From Hexcel Corporation IM7	0.5 wt.% amine f-SWNTs	E = 62-74, TS = 681-747	0.2-0.5 wt.%	[185]
PEEK	CNTs (armchair)	D = 0.678 nm, L = 2.951 nm or 4.92 nm	Molecular dynamics (MD)	E = 4,04 GPa ↑ 10% and interface properties	1 wt.%	[186]
PEEK	MWNTs	D variation	Fuseddeposition modeling (FDM)	TS slightly improved	1, 5 wt.%	[187]
PEEK	Bamboo MWNTs (B-	Commercially purchased, not	PEEK/B-CNT-Synthetic-Diamond composite	Coefficient of friction and specific wear rate	0.75-1 wt.%	[188]

	CNTs)	identified. High aspect ratio	was fabricated by a hot compression sintering technique	reduced by 30% and 39%		
PEEK-grafting	Acylated CNTs, and glass fibers (GFs)	D = 20-30 nm, L = 10-20 μm	GF/PEEK by immerse/stir, rinsed/dried, ····stacking	Interlaminar shear strength, TS, and E improved by 75%(~35 MPa), 23%(~338 MPa), 12% (~18 GPa), respectively	GFs ~40 vol.%	[189]
PEK-C/Tetrahydrofuran (THF)	MWNTs	Commercially purchased and intergratly laminated as sandwich	Ultrasonic homogenizer and laminated	G_{IC} and G_{IR} improved by 138.1% and 127.3%, respectively	PEK-C/THF 12 wt.%, PEK-C/CNTs 3 wt.%	[190]
PEK-C	MWNTs	Commercially purchased without identifying	Spin coating method for preparing interleaving film	Flexure strength and flexure modulus changes within 20%	0.1, 0.3, 0.5, 0.7 wt.%	[191]
PEEK	MWNTs	D ~40 nm, L ~30 μm	FEA based on RVE[§]	$\Delta U = (5.1, 1.3, 0.2) \times 10^{-10}$ mJ/cycle [§§] Max sliding zone length = (420, 290, 160) nm	1, 3, 10 vol.%	[90]
PEEK	MWNTs	D ~40 nm, L/D ~150	Shear lag analysis considering stick-slip	Nonlinear stress-strain curves, well agree to the experiments	6, 10 vol.%	[91]
PEEK	MWNTs	D ~40 nm, L/D ~100	Shear lag analysis considering stick-slip	Nonlinear stress-strain curve, stick-slip	6, 9 vol.%	[92]

				unloading behavior and critical interfacial shear strength, well agree to the experiments		
PAN	MWNTs	D = 15-20 nm, L/D = 55	Aligned PAN-graftred MWNTs	E 204.5%↑, TS 320.7%↑	2 wt.%	[38]
Epoxy	CNT bundles	Aligned CVD-CNTs	Hotcuring epoxy based on bishenol	E = 2.1-47.3, TS = 124.5-514	30 vol.%	[39]
PEHMA-co-UPyMA	MWNTs	DO = 20-40 nm, DI = 5-10 nm, L = 10-30 μm	Multiple H-bonding	E = 0.00564-0.068, TS >100%↑ ε_f 1054% ↑ at 4 wt.%	1.4-7.4 wt.%	[4]
PU	AO-MWNTs AA-MWNTs AU-MWNTs	DO = 10-30 nm	Acid oxidation coupled with a surpant	E = 0.170-0.270, TS = 26.6-63.4 at 1.8% MWNTs	0.18-10 wt.%	[5]

Note: *TS is the ultimate tensile strength (MPa). #ε_f is the elongation at break. ** K_{IC} is the mode-I fracture toughness. ***H is the hardness. @ Sy is the yield strength (MPa). @@CS is the compressive strength (MPa). [§] Finite element analysis (FEA) based on representative volumetric element (RVE). [§§] The dissipated energy per RVE.

3.4 Other Properties

The review so far has focused on the general electrical, thermal, and mechanical properties of CPCs and factors influencing them. In this subsection, recent advances in various fields/topics, such as applications in flexible and stretchable CNTs/polymer films for realizing high-performance strain and pressure sensors, and transparency in tough screens, are precented. Table 4 summarizes some additional properties of CPCs with various polymer matrices, different morphological CNT fillers and aspect ratios, fabrication processes, and percolation thresholds.

Table 4 The other properties of some CPCs from literatures.

Matrix	CNTs Filler	Aspect Ratio	Fabrication Process	Other Properties	Percolation Threshold	Ref.
Polyamide film	SWNTs		BuckyPearls™ from Nanotechnologies Inc.	Transparency 83-95%	0.1-0.2 wt.%	[109]
PEDOT	SWNTs-buckypaper		HiPCO and Electric arc discharge	Transparency 87%		[111]
N/A	SWNTs-buckypaper	By Iljin Nanotechnology, Inc.	Acid treatment	Transparency 70-80%	100%	[112]
Poly(allylamine hydrochloride)	MWNTs	D = 10-30 nm	CNTs by CVD, f-CNTs by oxidation	Transparency 70%	8 wt.%	[113]
PE	MWNTs	Film t = 250 nm	Inert particulate fillers $CaCo_3$, talc and wollastonite	Transparency 80%	0.8 vol.%	[116]
Cellulose paper	CNTs-buckypaper			Electromagnetic shielding 30-40 GHz, yet highly flexible	8.32 wt.%	[133]
Methyl/ethyl P(MMA-co-EMA)	CVD-MWNTs		f-CNT by Octadecylamine. Solution casting	*T_g from 89 to 106°C	10 wt.%	[133]
PVA	CVD-MWNTs		f-CNT by ferritin protein. Solution casting	T_g from 79 to 102°C	1.5 wt.%	[137]
PP	CNTs	D ~9.5 nm, L ~1.5 mm	Solid phase molding	EM shielding 48.3 dB at 2.2 mm thickness	5 wt.%	[127]
Polyurethane	MWNT-OH	D = 20-40 nm, L = substantial aspect ratio	Coating, 75%polyurethane/25%ethanol	Anticorrosion protective efficiency 99.5%	3.0 wt.%	[35]

Note: *T_g is the glass transition temperature.

4. Discussion

As can be seen from the data in the tables above, the material properties of the CNT-modified nanocomposites depend on many factors, including the type of CNT filler (morphology and aspect ratio of CNTs), fabrication process, functionalization type, and percentage of the CNT addition, etc. For example, the electrical conductivity generally increases with increasing CNT length, diameter, or number of CNT wall layers. There are similar trends for other properties. The fabrication processes have been adopted/chosen according to the material synthesis requirements. However, there is still a lack of quantitative analysis and comparison. The effects of these factors are usually not in a monotonically changing pattern (monotonically increasing or monotonically decreasing). There is usually an inflection point (threshold value) where the material performance is at a maximum or minimum point that can be fully accounted for when we conduct effective new/novel material design.

However, it is not yet fully quantitively clear how the chemical f-CNTs incorporating hydrogen bonding can effectively transfer the unique attributes exhibited by CNTs at the nanoscale to the macroscale, and it is vital to comprehensively understand the ways in which CNTs are added to polymer composites correlates with the mechanical, thermal, and electrical performance of CPCs. CPC material design involves the accurate prediction of desired material properties by manipulating the material system composition including hydrogen bonded f-CNTs, CNT morphology (chirality, number of wall layers, aspect ratio, etc.), CNT hydrogen bonding forms (end-to-end alignment or overlapping connections, etc.), the interactions among the constitutions and matrices based on chemical physics and materials science.

Depending on the problem and spatial and time scales of interest, various approaches to materials design based on computer modeling exist, from quantum mechanics to continuum simulations. Molecular dynamics (MD) or first principles simulations are ideal for studying nanoscale material properties. MD is an atomistic scale simulation that describes the interactions between atoms through interatomic potentials. In the MD method, electronic effects are averaged, and the time evolution of atomic positions and velocities is calculated from Newton's equations of motion. The electron-dependent approximation is based on the Born-Oppenheimer theory, and the MD time step used to describe atomic motion is long enough for electrons to achieve their ground stable state, as compared to nuclei due to mass differences. The interatomic potentials (force fields) are established from the first principles or experiment to describe the interactions between the atoms, including the effect of electrons, in terms of reproducible forces. The reliability of the interatomic potentials determines the accuracy of the MD simulations is furthermore related to the ability to bridge the effectiveness of mesoscale methods [40, 42, 192-197]. The polymer matrices and CNTs can interact through strong covalent or electrostatic interactions or hydrogen bonding. These chemical interactions lead to strong coupling at the interface. Alternatively, polymer matrices can interact with CNTs through weak electrostatic interactions, such as van der Waals forces [29, 198-201]. These detailed considerations are very important when considering the design and optimization of the load/electron/phonon transferring/passing through across the interface.

Because there are too many factors involved in the preparation, fabrication, and post-processing of the matrix, the CNT reinforcement, and the composite material, too complex and too strongly coupled, it is difficult to quantitatively draw the summary research results of this topic as each individual factor changes. Fortunately, there are some specific examples or case studies that can

demonstrate the effective applications of CNT-modified polymeric nanocomposites. Those findings were obtained by MD simulations, which outlines the effects of factors, such as CNT chirality, CNT length, CNT volume fraction, and CNT overlap length, individually on the thermal and electrical properties of CNTs and CNT-modified polymeric composites, respectively. Furthermore, those quantitative results provide tangible evidence for the potential of these materials and guidelines for material design [202].

5. Conclusions

CNTs are well-known nanofillers that can be used to produce high-performance polymer nanocomposites. The chemically f-CNTs, incorporating hydrogen bonding and appropriate solvents help to create well-dispersed CNT networks as electron pathways in polymer nanocomposites, in addition to extending the length of CNTs to enhance directional performance, and by proper design to create desired properties to fit desired applications and show promise in energy storage, energy harvesting, mobile phones, surface engineering, optical coatings, and integrated circuit chips. However, multiple factors and strong coupling among CNT nanofillers and matrix materials pose difficulties in designing and optimizing such CPCs using traditional experimental trial and error approaches. The lack of a comprehensive understanding the effects of the composition, f-CNTs nanofillers, hydrogen bonding, CNT alignment and morphology, and interactions between the constitutions, on the CPC performance limits both the knowledge of designing CPCs with desired properties and their potential applications. This paper presents research in recent two decades in the relative areas, including CNT-modified highly electrically and thermally conductive erosion-corrosion-resistive nanostructured composites, chemically f-NCTs, incorporating hydrogen bonding, and CNT directional alignment in a polymer matrix for reinforcement in mechanical, electrical, and thermal applications. However, to gain a comprehensive and quantitative understanding of the effects of these factors on the performance of CPCs, further studies by computer modeling, especially MD simulations, will be highly needed for effective new/novel material design and development.

Acknowledgments

This work was supported by the J. J. Lohr College of Engineering and Mechanical Engineering Department at South Dakota State University and are gratefully acknowledged.

Author Contributions

Conceptualization, Z.H. and H.H.; methodology, Z.H. and H.H.; investigation, Z.H. and H.H.; resources, Z.H. and H.H.; data curation, Z.H.; writing—original draft preparation, Z.H.; writing—review and editing, Z.H. and H.H.; visualization, Z.H.; project administration, Z.H. and H.H.; funding acquisition, H.H. All authors have read and agreed to the published version of the manuscript.

Funding

This research was fund through US Army Research Lab (Cooperative agreement W911NF15-2-0034-S).

Competing Interests

The authors declare no conflict of interest. The funders had no role in the design of the study; in the collection, analyses, or interpretation of data; in the writing of the manuscript; or in the decision to publish the results.

References

1. Byrne MT, Gun'ko YK. Recent advances in research on carbon nanotube–polymer composites. Adv Mater. 2010; 22: 1672-1688.
2. Fifield LS, Grate JW. Hydrogen-bond acidic functionalized carbon nanotubes (CNTs) with covalently-bound hexafluoroisopropanol groups. Carbon. 2010; 48: 2085-2088.
3. Ma PC, Siddiqui NA, Marom G, Kim JK. Dispersion and functionalization of carbon nanotubes for polymer-based nanocomposites: A review. Compos Part A. 2010; 41: 1345-1367.
4. Kokil A, Saito T, Depolo W, Elkins CL, Wilkes GL, Long TE. Introduction of multiple hydrogen bonding for enhanced mechanical performance of polymer-carbon nanotube composites. J Macromol Sci Part A. 2011; 48: 1016-1021.
5. Inglefield Jr DL, Bodnar RJ, Long TE. Hydrogen bond containing multiwalled carbon nanotubes in polyurethane composites. Polym Compos. 2016; 37: 1425-1434.
6. Mohd Nurazzi N, Asyraf MM, Khalina A, Abdullah N, Sabaruddin FA, Kamarudin SH, et al. Fabrication, functionalization, and application of carbon nanotube-reinforced polymer composite: An overview. Polymers. 2021; 13: 1047.
7. Lim JV, Bee ST, Tin Sin L, Ratnam CT, Abdul Hamid ZA. A review on the synthesis, properties, and utilities of functionalized carbon nanoparticles for polymer nanocomposites. Polymers. 2021; 13: 3547.
8. Sharma VP, Sharma U, Chattopadhyay M, Shukla VN. Advance applications of nanomaterials: A review. Mater Today. 2018; 5: 6376-6380.
9. Lee DK, Yoo J, Kim H, Kang BH, Park SH. Electrical and thermal properties of carbon nanotube polymer composites with various aspect ratios. Materials. 2022; 15: 1356.
10. de Oliveira AD, Beatrice CAG. Polymer nanocomposites with different types of nanofiller. In: Nanocomposites – Recent Evolutions. London, United Kingdom: IntechOpen; 2018.
11. Bikiaris DN. Nanocomposites with different types of nanofillers and advanced properties for several applications. Appl Nano. 2022; 3: 160-162.
12. Thulasi G, Kandampalayam PA, Rathanasamy R, Palaniappan SK, Palanisamy SK. Reduction of harmful nitrogen oxide emission from low heat rejection diesel engine using carbon nanotubes. Therm Sci. 2016; 20: 1181-1187.
13. Rathanasamy R, Sahoo S, Lee JH, Das AK, Somasundaram M, Palaniappan SK, et al. Carbon-based multi-layered films for electronic application: A review. J Electron Mater. 2021; 50: 1845-1892.
14. Chinnasamy M, Rathanasamy R, Palaniappan SK, Selvam S, Kaliyannan GV, Jaganathan S. Chapter-Hetero atom doped carbon nanomaterials for biological applications. In: Defect Engineering of Carbon Nanostructures. Advances in Material Research and Technology. Chem: Springer; 2022. pp. 35-59. doi: 10.1007/978-3-030-94375-2_2.
15. Raj MKA, Rathanasamy R, Palaniappan SK, Kaliyannan G, Chinnasamy M, Sivaraj S. Chapter-Heteroatom doping in nanocarbon and its applications. In: Defect Engineering of Carbon

Nanostructures. Advances in Material Research and Technology. Chem: Springer; 2022. pp. 61-81. doi: 10.1007/978-3-030-94375-2_3.

16. Kaliyannan GV, Rathanasamy R, Gunasekaran R, Anbupalani MS, Chinnasamy M, Palaniappan SK. Chapter-Doping of carbon nanostructures for energy application. In: Defect Engineering of Carbon Nanostructures. Advances in Material Research and Technology. Chem: Springer; 2022. pp. 83-109.
17. Palaniappan SK, Chinnasamy M, Rathanasamy R, Chinnasamy V, Sivaraj S. Chapter-Defected carbon nanotubes and their application. In: Defect Engineering of Carbon Nanostructures. Advances in Material Research and Technology. Chem: Springer; 2022. pp. 111-141. doi: 10.1007/978-3-030-94375-2_4.
18. Huang YY, Terentjev EM. Dispersion of carbon nanotubes: Mixing, sonication, stabilization, and composite properties. Polymers. 2012; 4: 275-295.
19. Pramanik C, Gissinger JR, Kumar S, Heinz H. Carbon nanotube dispersion in solvents and polymer solutions: Mechanisms, assembly, and preferences. ACS Nano. 2017; 11: 12805-12816.
20. Maity KP, Patra A, Prasad V. Influence of the chemical functionalization of carbon nanotubes on low temperature ac conductivity with polyaniline composites. J Phys D. 2020; 53: 125303.
21. Quintero-Jaime AF, Cazorla-Amorós D, Morallon E. Electrochemical functionalization of single wall carbon nanotubes with phosphorus and nitrogen species. Electrochim Acta. 2020; 340: 135935.
22. Nakonechna OI, Belyavina NN, Dashevskyi MM, Ivanenko KO, Revo SL. Novel Ti_2CuCx and Ti_3Cu_2Cx carbides obtained by sintering of products of mechanochemical synthesis of Ti, Cu and carbon nanotubes. Phys Chem Solid State. 2018; 19: 179-185.
23. Trulli MG, Sardella E, Palumbo F, Palazzo G, Giannossa LC, Mangone A, et al. Towards highly stable aqueous dispersions of multi-walled carbon nanotubes: The effect of oxygen plasma functionalization. J Colloid Interface Sci. 2017; 491: 255-264.
24. Norizan MN, Moklis MH, Demon SZ, Halim NA, Samsuri A, Mohamad IS, et al. Carbon nanotubes: Functionalisation and their application in chemical sensors. RSC Adv. 2020; 10: 43704-43732.
25. Jacobs CB, Peairs MJ, Venton BJ. Carbon nanotube based electrochemical sensors for biomolecules. Anal Chim Acta. 2010; 662: 105-127.
26. Spitalsky Z, Tasis D, Papagelis K, Galiotis C. Carbon nanotube–polymer composites: Chemistry, processing, mechanical and electrical properties. Prog Polym Sci. 2010; 35: 357-401.
27. Zhao YL, Stoddart JF. Noncovalent functionalization of single-walled carbon nanotubes. Acc Chem Res. 2009; 42: 1161-1171.
28. Konnola R, Joseph K. Effect of side-wall functionalisation of multi-walled carbon nanotubes on the thermo-mechanical properties of epoxy composites. RSC Adv. 2016; 6: 23887-23899.
29. Chen J, Yan L, Song W, Xu D. Interfacial characteristics of carbon nanotube-polymer composites: A review. Compos Part A. 2018; 114: 149-169.
30. Ajayan PM, Stephan O, Colliex C, Trauth D. Aligned carbon nanotube arrays formed by cutting a polymer resin—nanotube composite. Science. 1994; 265: 1212-1214.
31. Goh PS, Ismail AF, Ng BC. Directional alignment of carbon nanotubes in polymer matrices: Contemporary approaches and future advances. Compos Part A. 2014; 56: 103-126.
32. McClory C, Chin SJ, McNally T. Polymer/carbon nanotube composites. Aust J Chem. 2009; 62: 762-785.

33. Lou D, Younes H, Yang J, Jasthi BK, Hong G, Hong H, et al. Enhanced electrical conductivity of anticorrosive coatings by functionalized carbon nanotubes: Effect of hydrogen bonding. Nanotechnology. 2022; 33: 155704.
34. Christensen G, Yang J, Lou D, Hong G, Hong H, Tolle C, et al. Carbon nanotubes grease with high electrical conductivity. Synth Met. 2020; 268: 116496.
35. Younes H, Al-Rub RA, Rahman MM, Dalaq A, Al Ghaferi A, Shah T. Processing and property investigation of high-density carbon nanostructured papers with superior conductive and mechanical properties. Diam Relat Mater. 2016; 68: 109-117.
36. Ji J, Sui G, Yu Y, Liu Y, Lin Y, Du Z, et al. Significant improvement of mechanical properties observed in highly aligned carbon-nanotube-reinforced nanofibers. J Phys Chem C. 2009; 113: 4779-4785.
37. Bao JW, Cheng QF, Wang XP, Liang ZY, Wang B, Zhang C, et al. Mechanical properties of functionalized nanotube buckypaper composites. Proceedings of 17th International Conference on Composite Materials; 2009 July 27-31; Edinburgh, UK.
38. Mikhalchan A, Gspann T, Windle A. Aligned carbon nanotube–epoxy composites: The effect of nanotube organization on strength, stiffness, and toughness. J Mater Sci. 2016; 51: 10005-10025.
39. Tang Z, Huang Q, Liu Y, Chen Y, Guo B, Zhang L. Uniaxial stretching-induced alignment of carbon nanotubes in cross-linked elastomer enabled by dynamic cross-link reshuffling. ACS Macro Lett. 2019; 8: 1575-1581.
40. Jia D. Mechanical and thermal properties of two-dimensional material. Charlotte: The University of North Carolina; 2015.
41. Wang P, Cao Q, Wang H, Liu S, Chen Y, Peng Q. CNT-sandwiched copper composites as super thermal conductors for heat management. Physica E. 2021; 128: 114557.
42. He J. Molecular mechanisms and design of hydrogen-bonded materials for thermal applications. Logan: Utah State University; 2020.
43. Han Z, Fina A. Thermal conductivity of carbon nanotubes and their polymer nanocomposites: A review. Prog Polym Sci. 2011; 36: 914-944.
44. Che J, Cagin T, Goddard III WA. Thermal conductivity of carbon nanotubes. Nanotechnology. 2000; 11: 65.
45. Hone J, Llaguno MC, Biercuk MJ, Johnson AT, Batlogg B, Benes Z, et al. Thermal properties of carbon nanotubes and nanotube-based materials. Appl Phys A. 2002; 74: 339-343.
46. Zhang Q, Chen G, Yoon SF, Ahn J, Wang SG, Zhou Q, et al. Thermal conductivity of multiwalled carbon nanotubes. Phys Rev B. 2002; 66: 165440.
47. Marconnet AM, Panzer MA, Goodson KE. Thermal conduction phenomena in carbon nanotubes and related nanostructured materials. Rev Mod Phys. 2013; 85: 1295.
48. Bi K, Liu Y, Zhang C, Li J, Chen M, Chen Y. Thermal transport across symmetric and asymmetric solid–solid interfaces. Appl Phys A. 2016; 122: 883.
49. Shakhnov VA, Zinchenko LA, Makarchuk VV, Rezchikova EV, Kazakov VV. Visual analytics in investigation of chirality-dependent thermal properties of carbon nanotubes. J Phys. 2017; 829: 012008.
50. Younes H, Shoaib N, Rahman MM, Al-Rub RA, Hong H, Christensen G, et al. Thin carbon nanostructure mat with high electromagnetic interference shielding performance. Synth Met. 2019; 253: 48-56.
51. Christensen G, Younes H, Hong G, Lou D, Hong H, Widener C, et al. Hydrogen bonding enhanced

thermally conductive carbon nano grease. Synth Met. 2020; 259: 116213.
52. Lou D, Grablander T, Mao M, Hong H, Peterson GP. Improved thermal conductivity of PEG-based fluids using hydrogen bonding and long chain of nanoparticle. J Nanopart Res. 2021; 23: 98.
53. Christensen G, Lou D, Hong H, Peterson GP. Improved thermal conductivity of fluids and composites using boron nitride (BN) nanoparticles through hydrogen bonding. Thermochim Acta. 2021; 700: 178927.
54. Oluwalowo A, Nguyen N, Zhang S, Park JG, Liang R. Electrical and thermal conductivity improvement of carbon nanotube and silver composites. Carbon. 2019; 146: 224-231.
55. Chen J, Han J. Effect of hydroxylated carbon nanotubes on the thermal and electrical properties of derived epoxy composite materials. Res Phys. 2020; 18: 103246.
56. Jia Y, Yang J, Wang K, Chowdhury MA, Chen B, Su Y, et al. Aligned carbon nanotube/carbon (CNT/C) composites with exceptionally high electrical conductivity at elevated temperature to 400 C. Mater Res Express. 2019; 6: 116302.
57. Kanoun O, Bouhamed A, Ramalingame R, Bautista-Quijano JR, Rajendran D, Al-Hamry A. Review on conductive polymer/CNTs nanocomposites based flexible and stretchable strain and pressure sensors. Sensors. 2021; 21: 341.
58. Conley K, Karttunen AJ. Bridging the junction: Electrical conductivity of carbon nanotube networks. J Phys Chem C. 2022; 126: 17266-17274.
59. Wang Y, Lu S, He W, Gong S, Zhang Y, Zhao X, et al. Modeling and characterization of the electrical conductivity on metal nanoparticles/carbon nanotube/polymer composites. Sci Rep. 2022; 12: 10448.
60. Arnold MS, Green AA, Hulvat JF, Stupp SI, Hersam MC. Sorting carbon nanotubes by electronic structure using density differentiation. Nat Nanotechnol. 2006; 1: 60-65.
61. Grossiord N, Kivit PJ, Loos J, Meuldijk J, Kyrylyuk AV, van der Schoot P, et al. On the influence of the processing conditions on the performance of electrically conductive carbon nanotube/polymer nanocomposites. Polymer. 2008; 49: 2866-2872.
62. Jung YJ, Kar S, Talapatra S, Soldano C, Viswanathan G, Li X, et al. Aligned carbon nanotube−polymer hybrid architectures for diverse flexible electronic applications. Nano Lett. 2006; 6: 413-418.
63. Chen W, Tao X. Self-organizing alignment of carbon nanotubes in thermoplastic polyurethane. Macromol Rapid Commun. 2005; 26: 1763-1767.
64. Fischer JE, Zhou W, Vavro J, Llaguno MC, Guthy C, Haggenmueller R, et al. Magnetically aligned single wall carbon nanotube films: Preferred orientation and anisotropic transport properties. J Appl Phys. 2003; 93: 2157-2163.
65. Khan W, Sharma R, Saini P. Chapter 1-Carbon nanotube-based polymer composites: Synthesis, properties and applications. In: Carbon nanotubes-Current progress of their polymer composites. London, UK: Intech Open Science; 2016.
66. Azhari S, Yousefi AT, Tanaka H, Khajeh A, Kuredemus N, Bigdeli MM, et al. Fabrication of piezoresistive based pressure sensor via purified and functionalized CNTs/PDMS nanocomposite: Toward development of haptic sensors. Sens Actuator A. 2017; 266: 158-165.
67. Azizighannad S, Mitra S. Controlled synthesis of reduced graphene oxide-carbon nanotube hybrids and their aqueous behavior. J Nanopart Res. 2020; 22: 130.
68. McClory C, McNally T, Baxendale M, Pötschke P, Blau W, Ruether M. Electrical and rheological percolation of PMMA/MWCNT nanocomposites as a function of CNT geometry and

functionality. Eur Polym J. 2010; 46: 854-868.
69. Costa P, Silva J, Ansón-Casaos A, Martinez MT, Abad MJ, Viana J, et al. Effect of carbon nanotube type and functionalization on the electrical, thermal, mechanical and electromechanical properties of carbon nanotube/styrene–butadiene–styrene composites for large strain sensor applications. Compos Part B. 2014; 61: 136-146.
70. Bouhamed A, Rajendran D, Frenzel P, Zubkova T, Al-Hamry A, Miesel D, et al. Customizing hydrothermal properties of inkjet printed sensitive films by functionalization of carbon nanotubes. Nanotechnology. 2020; 32: 105708.
71. Dyke CA, Tour JM. Overcoming the insolubility of carbon nanotubes through high degrees of sidewall functionalization. Chem Eur J. 2004; 10: 812-817.
72. Zhu J, Kim J, Peng H, Margrave JL, Khabashesku VN, Barrera EV. Improving the dispersion and integration of single-walled carbon nanotubes in epoxy composites through functionalization. Nano Lett. 2003; 3: 1107-1113.
73. Yang QS, Li BQ, He XQ, Mai YW. Modeling the mechanical properties of functionalized carbon nanotubes and their composites: Design at the atomic level. Adv Condens Matter Phys. 2014; 2014: 482056.
74. Noordadi M, Mehrnejad F, Sajedi RH, Jafari M, Ranjbar B. The potential impact of carboxylic-functionalized multi-walled carbon nanotubes on trypsin: A Comprehensive spectroscopic and molecular dynamics simulation study. PLoS One. 2018; 13: e0198519.
75. Wolski P, Nieszporek K, Panczyk T. Pegylated and folic acid functionalized carbon nanotubes as pH controlled carriers of doxorubicin. Molecular dynamics analysis of the stability and drug release mechanism. Phys Chem Chem Phys. 2017; 19: 9300-9312.
76. Nicolle L, Journot CM, Gerber-Lemaire S. Chitosan functionalization: Covalent and non-covalent interactions and their characterization. Polymers. 2021; 13: 4118.
77. Dubey R, Dutta D, Sarkar A, Chattopadhyay P. Functionalized carbon nanotubes: Synthesis, properties and applications in water purification, drug delivery, and material and biomedical sciences. Nanoscale Adv. 2021; 3: 5722-5744.
78. Kumar MH, Mahalakshmi S, Kumar VM, Sathishkumar P, Moganapriya C, Rajasekar R. Chapter 6-Carbon polymer supports hybrid for alcohol oxidation. In: Nanomaterials for Alcohol Fuel Cells. Millersville: Materials Research Forum LLC.; 2019. doi: 10.21741/9781644900192.
79. Arunan E, Desiraju GR, Klein RA, Sadlej J, Scheiner S, Alkorta I, et al. Definition of the hydrogen bond (IUPAC Recommendations 2011). Pure Appl Chem. 2011; 83: 1637-1641.
80. Steiner T. The hydrogen bond in the solid state. Angew Chem Int Ed. 2002; 41: 48-76.
81. Nadi A, Boukhriss A, Bentis A, Jabrane E, Gmouh S. Evolution in the surface modification of textiles: A review. Text Prog. 2018; 50: 67-108.
82. Wikipedia. Hydrogen bond [Internet]. 2023 [cited date 2023 January 12]. Available from: https://en.wikipedia.org/wiki/Hydrogen_bond.
83. Jeffrey GA. An introduction to hydrogen bonding. New York, USA: Oxford university press; 1997.
84. Sweetman AM, Jarvis SP, Sang H, Lekkas I, Rahe P, Wang Y, et al. Mapping the force field of a hydrogen-bonded assembly. Nat Commun. 2014; 5: 3931.
85. Pimentel G, McClellan A. The hydrogen Bond. Franklin Classics Trade Press; 2018.
86. Kuo SW. Hydrogen bonding in polymeric materials. Hoboken, New Jersey, USA: John Wiley & Sons; 2018.
87. Li X, Ci L, Kar S, Soldano C, Kilpatrick SJ, Ajayan PM. Densified aligned carbon nanotube films via

vapor phase infiltration of carbon. Carbon. 2007; 45: 847-851.
88. Zhang RP, Zhu YF, Ma C, Liang J. Alignment of carbon nanotubes in poly (methyl methacrylate) composites induced by electric field. J Nanosci Nanotechnol. 2009; 9: 2887-2893.
89. Georgantzinos SK, Antoniou PA, Spitas C. A multi-scale computational framework for the hygro-thermo-mechanical analysis of laminated composite structures with carbon nanotube inclusions. Results Eng. 2023; 17: 100904.
90. Spitas V, Spitas C, Michelis P. Modeling of the elastic damping response of a carbon nanotube–polymer nanocomposite in the stress-strain domain using an elastic energy release approach based on stick-slip. Mech Adv Mater Struct. 2013; 20: 791-800.
91. Dwaikat MM, Spitas C, Spitas V. Predicting nonlinear stress–strain curves of unidirectional fibrous composites in consideration of stick–slip. Compos Part B. 2013; 44: 501-507.
92. Dwaikat MM, Spitas C, Spitas V. Effect of the stochastic nature of the constituents parameters on the predictability of the elastic properties of fibrous nano-composites. Compos Sci Technol. 2012; 72: 1882-1891.
93. Dwaikat MM, Spitas C, Spitas V. A model for elastic hysteresis of unidirectional fibrous nano composites incorporating stick-slip. Mater Sci Eng. 2011; 530: 349-356.
94. Huang H, Liu CH, Wu Y, Fan S. Aligned carbon nanotube composite films for thermal management. Adv Mater. 2005; 17: 1652-1656.
95. De Heer WA, Bacsa WS, Chatelain A, Gerfin T, Humphrey-Baker R, Forro L, et al. Aligned carbon nanotube films: Production and optical and electronic properties. Science. 1995; 268: 845-847.
96. Andrews R, Jacques D, Rao AM, Derbyshire F, Qian D, Fan X, et al. Continuous production of aligned carbon nanotubes: A step closer to commercial realization. Chem Phys Lett. 1999; 303: 467-474.
97. Gong QM, Li Z, Li D, Bai XD, Liang J. Fabrication and structure: A study of aligned carbon nanotube/carbon nanocomposites. Solid State Commun. 2004; 131: 399-404.
98. Gong QM, Li Z, Bai XD, Li D, Zhao Y, Liang J. Thermal properties of aligned carbon nanotube/carbon nanocomposites. Mater Sci Eng. 2004; 384: 209-214.
99. Wang L, Nygren G, Karkkainen RL, Yang Q. A multiscale approach for virtual testing of highly aligned short carbon fiber composites. Compos Struct. 2019; 230: 111462.
100. Jung S, Choi HW, Mocanu FC, Shin DW, Chowdhury MF, Han SD, et al. Modeling electrical percolation to optimize the electromechanical properties of CNT/polymer composites in highly stretchable fiber strain sensors. Sci Rep. 2019; 9: 20376.
101. Abazine K, Anakiou H, El Hasnaoui M, Graça MP, Fonseca MA, Costa LC, et al. Electrical conductivity of multiwalled carbon nanotubes/polyester polymer nanocomposites. J Compos Mater. 2016; 50: 3283-3290.
102. Liu H, Gao J, Huang W, Dai K, Zheng G, Liu C, et al. Electrically conductive strain sensing polyurethane nanocomposites with synergistic carbon nanotubes and graphene bifillers. Nanoscale. 2016; 8: 12977-12989.
103. Gardea F, Lagoudas DC. Characterization of electrical and thermal properties of carbon nanotube/epoxy composites. Compos Part B. 2014; 56: 611-620.
104. Georgousis G, Pandis C, Kalamiotis A, Georgiopoulos P, Kyritsis A, Kontou E, et al. Strain sensing in polymer/carbon nanotube composites by electrical resistance measurement. Procedia Eng. 2012; 47: 774-777.
105. Pham GT, Park YB, Liang Z, Zhang C, Wang B. Processing and modeling of conductive

thermoplastic/carbon nanotube films for strain sensing. Compos Part B. 2008; 39: 209-216.
106. Geng Y, Liu MY, Li J, Shi XM, Kim JK. Effects of surfactant treatment on mechanical and electrical properties of CNT/epoxy nanocomposites. Compos Part A. 2008; 39: 1876-1883.
107. Du F, Fischer JE, Winey KI. Effect of nanotube alignment on percolation conductivity in carbon nanotube/polymer composites. Phys Rev B. 2005; 72: 121404.
108. Tchmutin IA, Ponomarenko AT, Krinichnaya EP, Kozub GI, Efimov ON. Electrical properties of composites based on conjugated polymers and conductive fillers. Carbon. 2003; 41: 1391-1395.
109. Watson KA, Ghose S, Delozier DM, Smith Jr JG, Connell JW. Transparent, flexible, conductive carbon nanotube coatings for electrostatic charge mitigation. Polymer. 2005; 46: 2076-2085.
110. Carroll DL, Czerw R, Webster S. Polymer–nanotube composites for transparent, conducting thin films. Synth Met. 2005; 155: 694-697.
111. Zhang D, Ryu K, Liu X, Polikarpov E, Ly J, Tompson ME, et al. Transparent, conductive, and flexible carbon nanotube films and their application in organic light-emitting diodes. Nano Lett. 2006; 6: 1880-1886.
112. Geng HZ, Kim KK, So KP, Lee YS, Chang Y, Lee YH. Effect of acid treatment on carbon nanotube-based flexible transparent conducting films. J Am Chem Soc. 2007; 129: 7758-7759.
113. Park HJ, Kim J, Chang JY, Theato P. Preparation of transparent conductive multilayered films using active pentafluorophenyl ester modified multiwalled carbon nanotubes. Langmuir. 2008; 24: 10467-10473.
114. Shim BS, Chen W, Doty C, Xu C, Kotov NA. Smart electronic yarns and wearable fabrics for human biomonitoring made by carbon nanotube coating with polyelectrolytes. Nano Lett. 2008; 8: 4151-4157.
115. O'Connor I, De S, Coleman JN, Gun'ko YK. Development of transparent, conducting composites by surface infiltration of nanotubes into commercial polymer films. Carbon. 2009; 47: 1983-1988.
116. Wang X, Wu P. Fluorinated carbon nanotube/nanofibrillated cellulose composite film with enhanced toughness, superior thermal conductivity, and electrical insulation. ACS Appl Mater Interfaces. 2018; 10: 34311-34321.
117. Shiyanova K, Gudkov M, Torkunov M, Ryvkina N, Chmutin I, Goncharuk G, et al. Segregated structure copolymer of vinylidene fluoride and tetrafluoroethylene composites filled with rGO, SWCNTs and their mixtures. Polymers. 2022; 14: 4105.
118. Pötschke P, Bhattacharyya AR, Janke A, Goering H. Melt mixing of polycarbonate/multi-wall carbon nanotube composites. Compos Interfaces. 2003; 10: 389-404.
119. Coleman JN, Blau WJ, Dalton AB, Munoz E, Collins S, Kim BG, et al. Improving the mechanical properties of single-walled carbon nanotube sheets by intercalation of polymeric adhesives. Appl Phys Lett. 2003; 82: 1682-1684.
120. Yang BX, Pramoda KP, Xu GQ, Goh SH. Mechanical reinforcement of polyethylene using polyethylene-grafted multiwalled carbon nanotubes. Adv Funct Mater. 2007; 17: 2062-2069.
121. Arash B, Wang Q, Varadan VK. Mechanical properties of carbon nanotube/polymer composites. Sci Rep. 2014; 4: 6479.
122. Choi EY, Kim JY, Kim CK. Fabrication and properties of polycarbonate composites with polycarbonate grafted multi-walled carbon nanotubes by reactive extrusion. Polymer. 2015; 60: 18-25.
123. Verma P, Saini P, Choudhary V. Designing of carbon nanotube/polymer composites using melt

recirculation approach: Effect of aspect ratio on mechanical, electrical and EMI shielding response. Mater Des. 2015; 88: 269-277.
124. Coleman JN, Khan U, Gun'ko YK. Mechanical reinforcement of polymers using carbon nanotubes. Adv Mater. 2006; 18: 689-706.
125. Alam J, Khan A, Alam M, Mohan R. Electroactive shape memory property of a Cu-decorated CNT dispersed PLA/ESO nanocomposite. Materials. 2015; 8: 6391-6400.
126. Hajializadeh S, Barikani M, Bellah SM. Synthesis and characterization of multiwall carbon nanotube/waterborne polyurethane nanocomposites. Polym Int. 2017; 66: 1074-1083.
127. Wu HY, Jia LC, Yan DX, Gao JF, Zhang XP, Ren PG, et al. Simultaneously improved electromagnetic interference shielding and mechanical performance of segregated carbon nanotube/polypropylene composite via solid phase molding. Compos Sci Technol. 2018; 156: 87-94.
128. Chen Y, Wei W, Zhu Y, Luo J, Liu X. Noncovalent functionalization of carbon nanotubes via co-deposition of tannic acid and polyethyleneimine for reinforcement and conductivity improvement in epoxy composite. Compos Sci Technol. 2019; 170: 25-33.
129. Mohiuddin M, Hoa SV. Temperature dependent electrical conductivity of CNT–PEEK composites. Compos Sci Technol. 2011; 72:21-27.
130. Mohiuddin M, Hoa SV. Estimation of contact resistance and its effect on electrical conductivity of CNT/PEEK composites. Compos Sci Technol. 2013; 79: 42-48.
131. Trakakis G, Tomara G, Datsyuk V, Sygellou L, Bakolas A, Tasis D, et al. Mechanical, electrical, and thermal properties of carbon nanotube buckypapers/epoxy nanocomposites produced by oxidized and epoxidized nanotubes. Materials. 2020; 13: 4308.
132. Guo H, Liu J, Wang Q, Liu M, Du C, Li B, et al. High thermal conductive poly (vinylidene fluoride)-based composites with well-dispersed carbon nanotubes/graphene three-dimensional network structure via reduced interfacial thermal resistance. Compos Sci Technol. 2019; 181: 107713.
133. Yang J, Hu J, Wang C, Qin Y, Guo Z. Fabrication and characterization of soluble multi-walled carbon nanotubes reinforced P (MMA-co-EMA) composites. Macromol Mater Eng. 2004; 289: 828-832.
134. Zhu J, Peng H, Rodriguez-Macias F, Margrave JL, Khabashesku VN, Imam AM, et al. Reinforcing epoxy polymer composites through covalent integration of functionalized nanotubes. Adv Funct Mater. 2004; 14: 643-648.
135. Gao J, Itkis ME, Yu A, Bekyarova E, Zhao B, Haddon RC. Continuous spinning of a single-walled carbon nanotube−nylon composite fiber. J Am Chem Soc. 2005; 127: 3847-3854.
136. Liu L, Barber AH, Nuriel S, Wagner HD. Mechanical properties of functionalized single-walled carbon-nanotube/poly (vinyl alcohol) nanocomposites. Adv Funct Mater. 2005; 15: 975-980.
137. Bhattacharyya S, Sinturel C, Salvetat JP, Saboungi ML. Protein-functionalized carbon nanotube-polymer composites. Appl Phys Lett. 2005; 86: 113104.
138. Eitan A, Fisher FT, Andrews R, Brinson LC, Schadler LS. Reinforcement mechanisms in MWCNT-filled polycarbonate. Compos Sci Technol. 2006; 66: 1162-1173.
139. Gorga RE, Lau KK, Gleason KK, Cohen RE. The importance of interfacial design at the carbon nanotube/polymer composite interface. J Appl Polym Sci. 2006; 102: 1413-1418.
140. Blake R, Coleman JN, Byrne MT, McCarthy JE, Perova TS, Blau WJ, et al. Reinforcement of poly (vinyl chloride) and polystyrene using chlorinated polypropylene grafted carbon nanotubes. J Mater Chem. 2006; 16: 4206-4213.

141. Rasheed A, Chae HG, Kumar S, Dadmun MD. Polymer nanotube nanocomposites: Correlating intermolecular interaction to ultimate properties. Polymer. 2006; 47: 4734-4741.
142. Sahoo NG, Jung YC, Yoo HJ, Cho JW. Effect of functionalized carbon nanotubes on molecular interaction and properties of polyurethane composites. Macromol Chem Phys. 2006; 207: 1773-1780.
143. Blond D, McCarthy DN, Blau WJ, Coleman JN. Toughening of artificial silk by incorporation of carbon nanotubes. Biomacromolecules. 2007; 8: 3973-3976.
144. Sun L, Warren GL, O'reilly JY, Everett WN, Lee SM, Davis D, et al. Mechanical properties of surface-functionalized SWCNT/epoxy composites. Carbon. 2008; 46: 320-328.
145. O'Connor I, Hayden H, O'Connor S, Coleman JN, Gun'ko YK. Kevlar coated carbon nanotubes for reinforcement of polyvinylchloride. J Mater Chem. 2008; 18: 5585-5588.
146. Li S, Wang F, Wang Y, Wang J, Ma J, Xiao J. Effect of acid and TETA modification on mechanical properties of MWCNTs/epoxy composites. J Mater Sci. 2008; 43: 2653-2658.
147. Byrne MT, McNamee WP, Gun'ko YK. Chemical functionalization of carbon nanotubes for the mechanical reinforcement of polystyrene composites. Nanotechnology. 2008; 19: 415707.
148. Qian D, Dickey EC, Andrews R, Rantell T. Load transfer and deformation mechanisms in carbon nanotube-polystyrene composites. Appl Phys Lett. 2000; 76: 2868-2870.
149. Cadek M, Coleman JN, Barron V, Hedicke K, Blau WJ. Morphological and mechanical properties of carbon-nanotube-reinforced semicrystalline and amorphous polymer composites. Appl Phys Lett. 2002; 81: 5123-5125.
150. Dufresne A, Paillet M, Putaux JL, Canet R, Carmona F, Delhaes P, et al. Processing and characterization of carbon nanotube/poly (styrene-co-butyl acrylate) nanocomposites. J Mater Sci. 2002; 37: 3915-3923.
151. Safadi B, Andrews R, Grulke EA. Multiwalled carbon nanotube polymer composites: Synthesis and characterization of thin films. J Appl Polym Sci. 2002; 84: 2660-2669.
152. Ruan SL, Gao P, Yang XG, Yu TX. Toughening high performance ultrahigh molecular weight polyethylene using multiwalled carbon nanotubes. Polymer. 2003; 44: 5643-5654.
153. Cadek M, Coleman JN, Ryan KP, Nicolosi V, Bister G, Fonseca A, et al. Reinforcement of polymers with carbon nanotubes: The role of nanotube surface area. Nano Lett. 2004; 4: 353-356.
154. Coleman JN, Cadek M, Blake R, Nicolosi V, Ryan KP, Belton C, et al. High performance nanotube-reinforced plastics: Understanding the mechanism of strength increase. Adv Funct Mater. 2004; 14: 791-798.
155. Chang TE, Kisliuk A, Rhodes SM, Brittain WJ, Sokolov AP. Conductivity and mechanical properties of well-dispersed single-wall carbon nanotube/polystyrene composite. Polymer. 2006; 47: 7740-7746.
156. Bakshi SR, Tercero JE, Agarwal A. Synthesis and characterization of multiwalled carbon nanotube reinforced ultra high molecular weight polyethylene composite by electrostatic spraying technique. Compos Part A. 2007; 38: 2493-2499.
157. Yun SI, Gadd GE, Latella BA, Lo V, Russell RA, Holden PJ. Mechanical properties of biodegradable polyhydroxyalkanoates/single wall carbon nanotube nanocomposite films. Polym Bull. 2008; 61: 267-275.
158. Jin Z, Pramoda KP, Xu G, Goh SH. Dynamic mechanical behavior of melt-processed multi-walled carbon nanotube/poly (methyl methacrylate) composites. Chem Phys Lett. 2001; 337: 43-47.
159. Thostenson ET, Chou TW. Aligned multi-walled carbon nanotube-reinforced composites:

Processing and mechanical characterization. J Phys D. 2002; 35: L77.
160. Gorga RE, Cohen RE. Toughness enhancements in poly (methyl methacrylate) by addition of oriented multiwall carbon nanotubes. J Polym Sci Part B. 2004; 42: 2690-2702.
161. Meincke O, Kaempfer D, Weickmann H, Friedrich C, Vathauer M, Warth H. Mechanical properties and electrical conductivity of carbon-nanotube filled polyamide-6 and its blends with acrylonitrile/butadiene/styrene. Polymer. 2004; 45: 739-748.
162. Liu IYP, Shen L, Chow SY, Zhang WD. Morphology and mechanical properties of multiwalled carbon nanotubes reinforced nylon-6 composites. Macromolecules. 2004; 37: 7214-7222.
163. Manchado ML, Valentini L, Biagiotti J, Kenny JM. Thermal and mechanical properties of single-walled carbon nanotubes–polypropylene composites prepared by melt processing. Carbon. 2005; 43: 1499-1505.
164. Kumar S, Dang TD, Arnold FE, Bhattacharyya AR, Min BG, Zhang X, et al. Synthesis, structure, and properties of PBO/SWNT Composites&. Macromolecules. 2002; 35: 9039-9043.
165. Velasco-Santos C, Martínez-Hernández AL, Fisher FT, Ruoff R, Castano VM. Improvement of thermal and mechanical properties of carbon nanotube composites through chemical functionalization. Chem Mater. 2003; 15: 4470-4475.
166. Blond D, Barron V, Ruether M, Ryan KP, Nicolosi V, Blau WJ, et al. Enhancement of modulus, strength, and toughness in poly (methyl methacrylate)-based composites by the incorporation of poly (methyl methacrylate)-functionalized nanotubes. Adv Funct Mater. 2006; 16: 1608-1614.
167. Yu A, Hu H, Bekyarova E, Itkis ME, Gao J, Zhao B, et al. Incorporation of highly dispersed single-walled carbon nanotubes in a polyimide matrix. Compos Sci Technol. 2006; 66: 1190-1197.
168. McIntosh D, Khabashesku VN, Barrera EV. Benzoyl peroxide initiated in situ functionalization, processing, and mechanical properties of single-walled carbon nanotube−polypropylene composite fibers. J Phys Chem C. 2007; 111: 1592-1600.
169. Kovalchuk AA, Shevchenko VG, Shchegolikhin AN, Nedorezova PM, Klyamkina AN, Aladyshev AM. Isotactic and syndiotactic polypropylene/multi-wall carbon nanotube composites: Synthesis and properties. J Mater Sci. 2008; 43: 7132-7140.
170. Bao JW, Cheng QF, Wang XP, Liang ZY, Wang B, Zhang C, et al. Mechanical properties of functionalized nanotube buckypaper composites. Compos Part A. 2004; 35: 1225.
171. Pham GT, Park YB, Wang S, Liang Z, Wang B, Zhang C, et al. Mechanical and electrical properties of polycarbonate nanotube buckypaper composite sheets. Nanotechnology. 2008; 19: 325705.
172. Blighe FM, Blau WJ, Coleman JN. Towards tough, yet stiff, composites by filling an elastomer with single-walled nanotubes at very high loading levels. Nanotechnology. 2008; 19: 415709.
173. Wang S, Liang Z, Pham G, Park YB, Wang B, Zhang C, et al. Controlled nanostructure and high loading of single-walled carbon nanotubes reinforced polycarbonate composite. Nanotechnology. 2007; 18: 095708.
174. Meng H, Sui GX, Fang PF, Yang R. Effects of acid-and diamine-modified MWNTs on the mechanical properties and crystallization behavior of polyamide 6. Polymer. 2008; 49: 610-620.
175. Yang BX, Shi JH, Li X, Pramoda KP, Goh SH. Mechanical reinforcement of poly (1-butene) using polypropylene-grafted multiwalled carbon nanotubes. J Appl Polym Sci. 2009; 113: 1165-1172.
176. Sui G, Zhong WH, Yang XP, Yu YH. Curing kinetics and mechanical behavior of natural rubber reinforced with pretreated carbon nanotubes. Mater Sci Eng. 2008; 485: 524-531.
177. Jiang Q, Wang X, Zhu Y, Hui D, Qiu Y. Mechanical, electrical and thermal properties of aligned carbon nanotube/polyimide composites. Compos Part B. 2014; 56: 408-412.

178. Xiang D, Harkin-Jones E, Linton D, Martin P. Structure, mechanical, and electrical properties of high-density polyethylene/multi-walled carbon nanotube composites processed by compression molding and blown film extrusion. J Appl Polym Sci. 2015; 132. doi: 10.1002/app.42665.
179. Mei H, Xia J, Han D, Xiao S, Deng J, Cheng L. Dramatic increase in electrical conductivity in epoxy composites with uni-directionally oriented laminae of carbon nanotubes. Chem Eng J. 2016; 304: 970-976.
180. Shamsi R, Mahyari M, Koosha M. Synthesis of CNT-polyurethane nanocomposites using ester-based polyols with different molecular structure: Mechanical, thermal, and electrical properties. J Appl Polym Sci. 2017; 134. doi: 10.1002/app.44567.
181. Deplancke T, Lame O, Barrau S, Ravi K, Dalmas F. Impact of carbon nanotube prelocalization on the ultra-low electrical percolation threshold and on the mechanical behavior of sintered UHMWPE-based nanocomposites. Polymer. 2017; 111: 204-213.
182. Martinez-Rubi Y, Ashrafi B, Jakubinek MB, Zou S, Laqua K, Barnes M, et al. Fabrication of high content carbon nanotube–Polyurethane sheets with tailorable properties. ACS Appl Mater Interfaces. 2017; 9: 30840-30849.
183. Yakovlev YV, Gagolkina ZO, Lobko EV, Khalakhan I, Klepko VV. The effect of catalyst addition on the structure, electrical and mechanical properties of the cross-linked polyurethane/carbon nanotube composites. Compos Sci Technol. 2017; 144: 208-214.
184. Kalakonda P, Banne S. Thermomechanical properties of PMMA and modified SWCNT composites. Nanotechnol Sci Appl. 2017; 10: 45-52.
185. Davis DC, Wilkerson JW, Zhu J, Hadjiev VG. A strategy for improving mechanical properties of a fiber reinforced epoxy composite using functionalized carbon nanotubes. Compos Sci Technol. 2011; 71: 1089-1097.
186. Wang B, Zhang K, Zhou C, Ren M, Gu Y, Li T. Engineering the mechanical properties of CNT/PEEK nanocomposites. RSC Adv. 2019; 9: 12836-12845.
187. Berretta S, Davies R, Shyng YT, Wang Y, Ghita O. Fused Deposition Modelling of high temperature polymers: Exploring CNT PEEK composites. Polym Test. 2017; 63: 251-262.
188. Vishal K, Rajkumar K, Annamalai VE. Wear and tribofilm characterization of bamboo CNT (B-CNT)-peek composite with incremental blending of submicron synthetic diamond particles. Wear. 2021; 466: 203556.
189. Zhu S, Qian Y, Hassan EA, Shi R, Yang L, Cao H, et al. Enhanced interfacial interactions by PEEK-grafting and coupling of acylated CNT for GF/PEEK composites. Compos Commun. 2020; 18: 43-48.
190. Yao J, Li H, Wu Y, Niu K. Establishment of interlaminar structure and crack propagation in carbon fiber reinforced epoxy composites by interleaving CNTs/PEK-C film. Fatigue Fract Eng Mater Struct. 2022; 45: 3347-360.
191. Yao J, Chang H, Zhang T, Niu Y. Synergistic toughening in the interleaved carbon fibre reinforced epoxy composites by thermoplastic resin and nanomaterials. Polym Test. 2022; 115: 107769.
192. Hernandez CAS. Molecular dynamic simulation of thermo-mechanical properties of ultra-thin poly (methyl methacrylate) films. College Station, TX: Texas A&M University; 2010.
193. Tallury SS, Pasquinelli MA. Molecular dynamics simulations of polymers with stiff backbones interacting with single-walled carbon nanotubes. J Phys Chem B. 2010; 114: 9349-9355.
194. Tallury SS, Pasquinelli MA. Molecular dynamics simulations of flexible polymer chains wrapping

single-walled carbon nanotubes. J Phys Chem B. 2010; 114: 4122-4129.
195. Eslami H, Mohammadzadeh L, Mehdipour N. Reverse nonequilibrium molecular dynamics simulation of thermal conductivity in nanoconfined polyamide-6, 6. J Chem Phys. 2011; 135: 064703.
196. Kim YJ. CNT-reinforced polymer nanocomposite by molecular dynamics simulations. West Lafayette, Indiana, USA: Purdue University; 2014.
197. Kumar U, Sharma S, Rathi R, Kapur S, Upadhyay D. Molecular dynamics simulation of nylon/CNT composites. Mater Today. 2018; 5: 27710-27717.
198. Gaikwad PS, Kowalik M, Jensen BD, Van Duin A, Odegard GM. Molecular dynamics modeling of interfacial interactions between flattened carbon nanotubes and amorphous carbon: Implications for ultra-lightweight composites. ACS Appl Nano Mater. 2022; 5: 5915-5924.
199. Eitan A, Jiang K, Dukes D, Andrews R, Schadler LS. Surface modification of multiwalled carbon nanotubes: Toward the tailoring of the interface in polymer composites. Chem Mater. 2003; 15: 3198-3201.
200. Eitan AA. Nanotube-polymer composites: Tailoring the interface for improved mechanical properties. Troy, NY, USA: Rensselaer Polytechnic Institute; 2004.
201. Mugadza K, Mombeshora ET, Stark A, Ndungu PG, Nyamori VO. Surface modifications of carbon nanotubes towards tailored electrochemical characteristics. J Mater Sci. 2021; 32: 27923-27936.
202. Najmi L, Hu Z. Review on Molecular Dynamics Simulations of Effects of Carbon Nanotubes (CNTs) on Electrical and Thermal Conductivities of CNT-Modified Polymeric Composites. J Compos Sci. 2023; 7: 165.